Dynamics of Astrophysical Jets

Nektarios Vlahakis
University of Athens

Outline

- introduction (observed jet characteristics)
- magnetohydrodynamics (collimation-acceleration)
- linear jet stability (resulting growth rates)

Examples of astrophysical jets

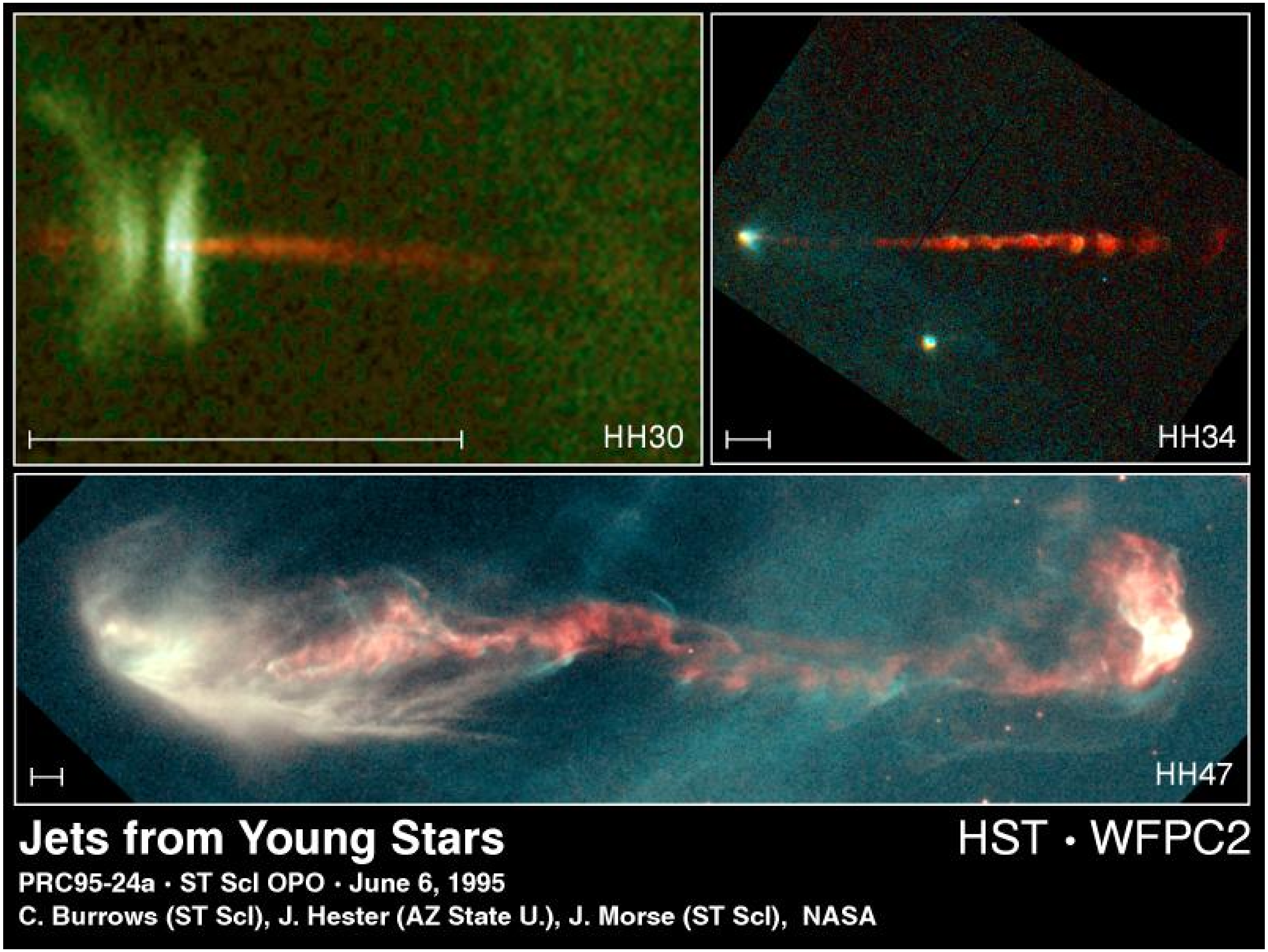

(scale =1000 AU, $V_\infty = a few 100$km/s)

The jet from the M87 galaxy

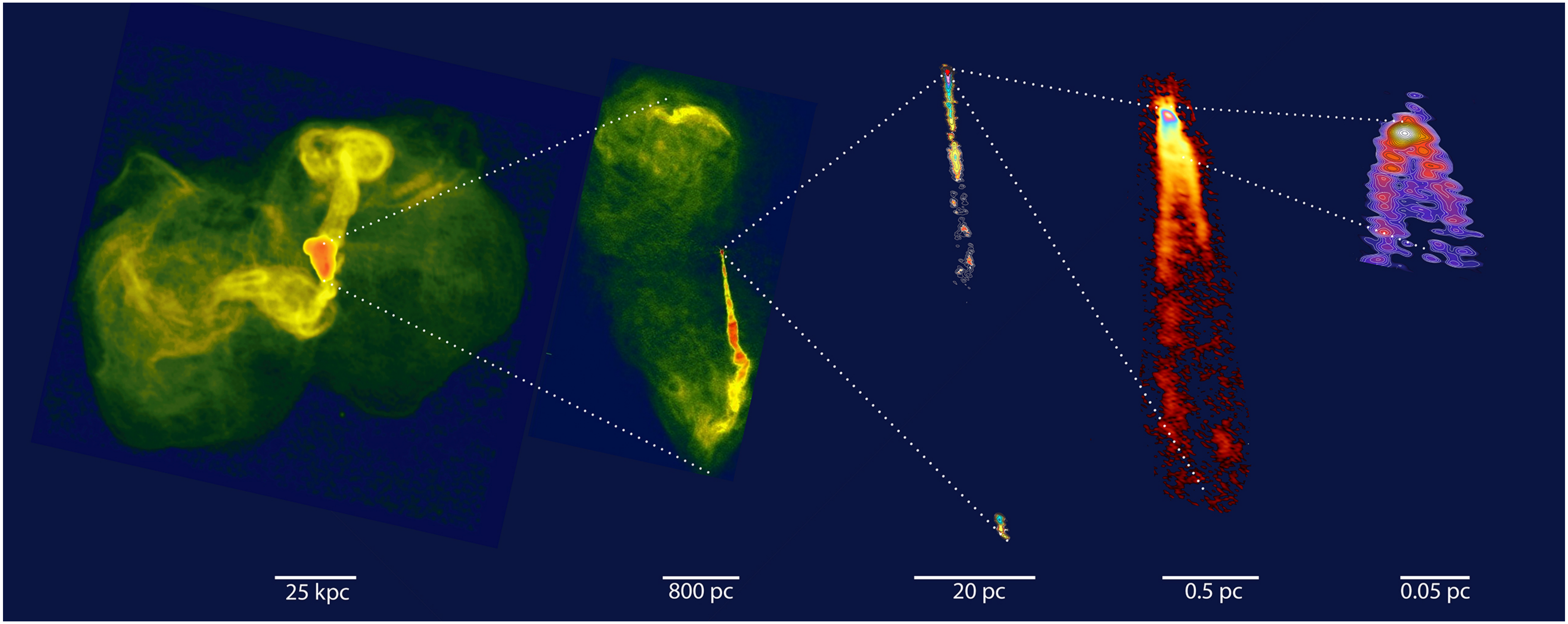

(from Blandford+2018)

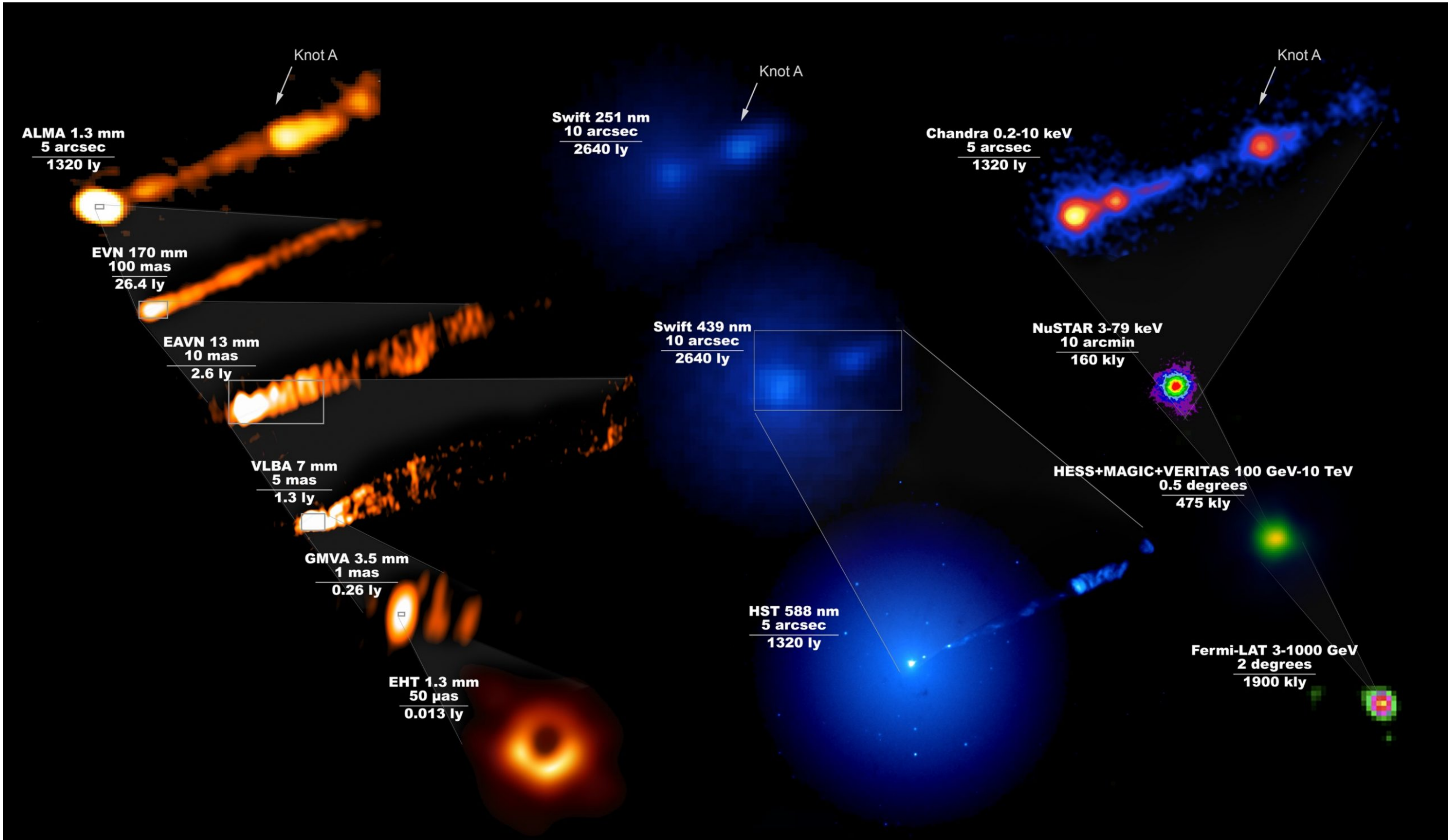

Image Credit: The EHT Multi-wavelength Science Working Group; the EHT Collaboration; ALMA (ESO/NAOJ/NRAO); the EVN; the EAVN Collaboration; VLBA (NRAO); the GMVA; the Hubble Space Telescope; the Neil Gehrels Swift Observatory; the Chandra X-ray Observatory; the Nuclear Spectroscopic Telescope Array; the Fermi-LAT Collaboration; the H.E.S.S collaboration; the MAGIC collaboration; the VERITAS collaboration; NASA and ESA. Composition by J. C. Algaba

Jet speed

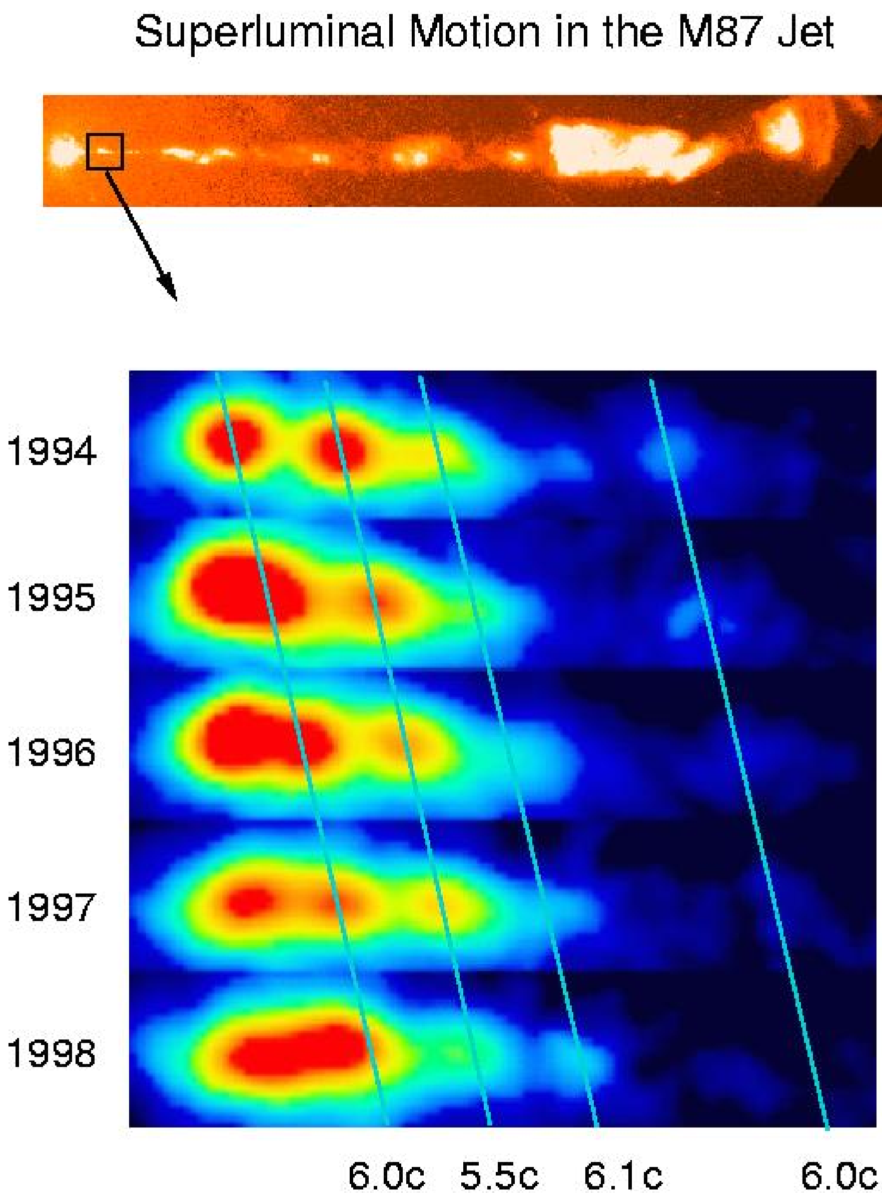

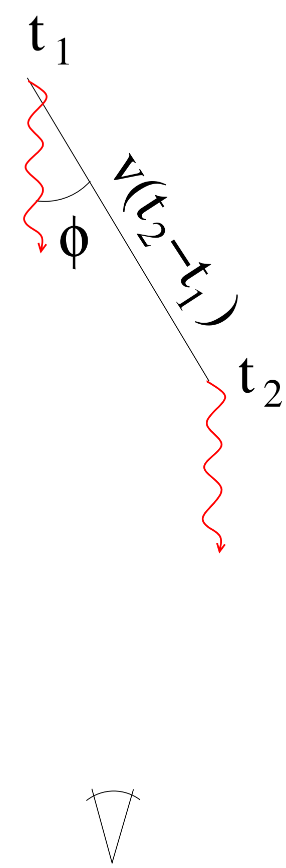

$$\gamma_\infty \sim 10$$

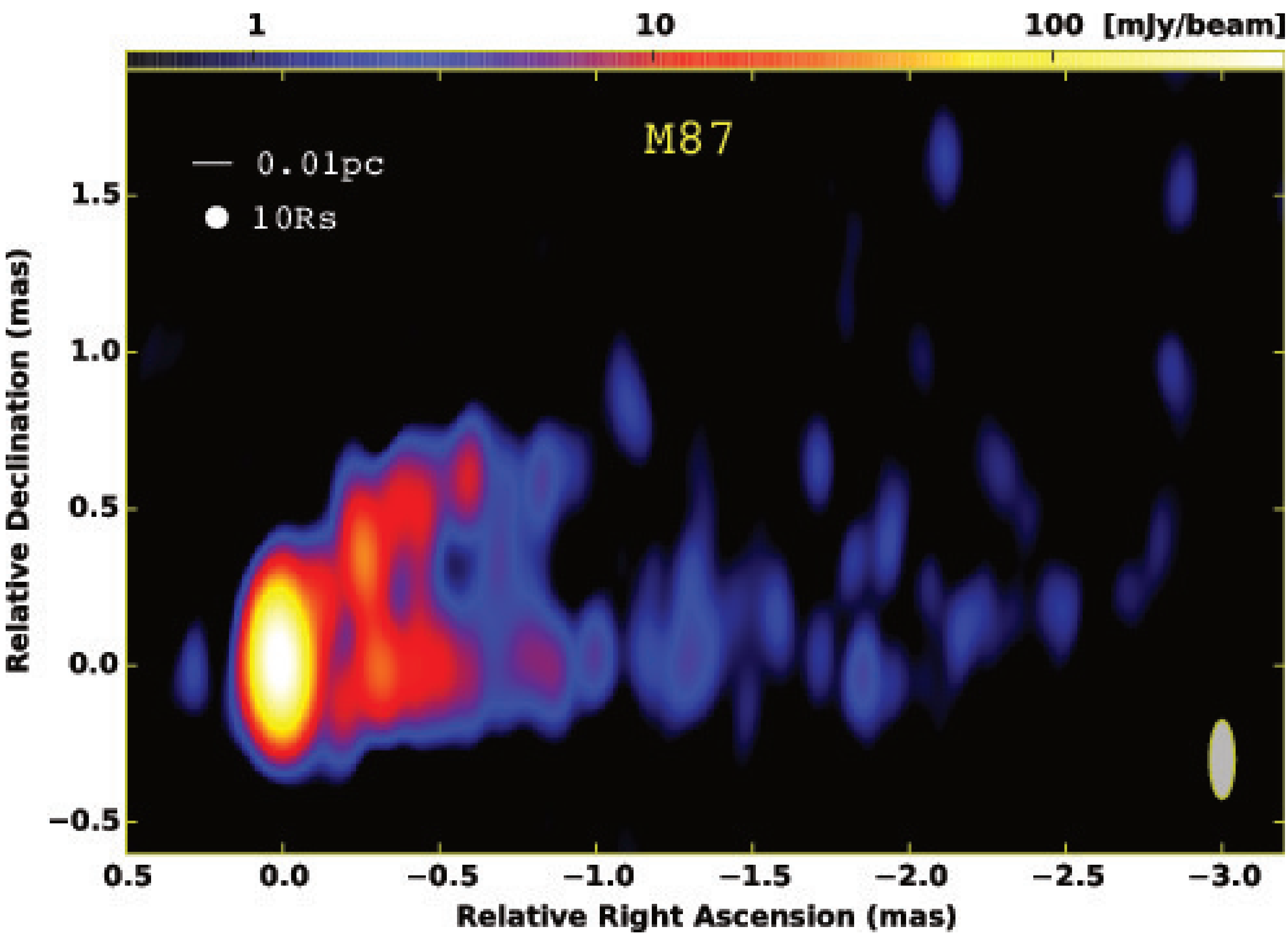

(Hada et al 2016)

collimation at $\sim$100 Schwarzschild radii

The jet shape (Nakamura & Asada 2013)

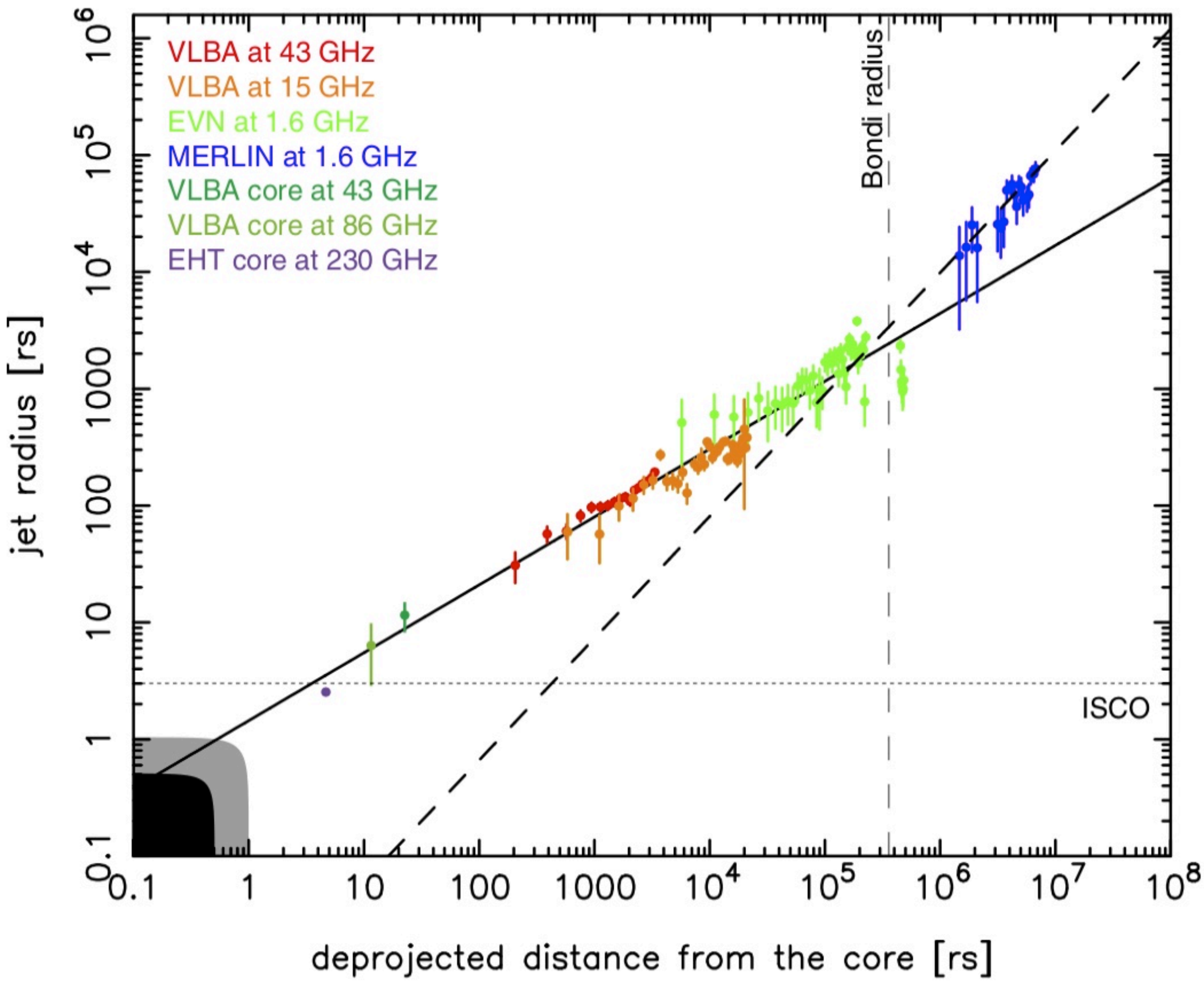

Parabolic up to the Bondi radius, then radial

(Hada+2013)

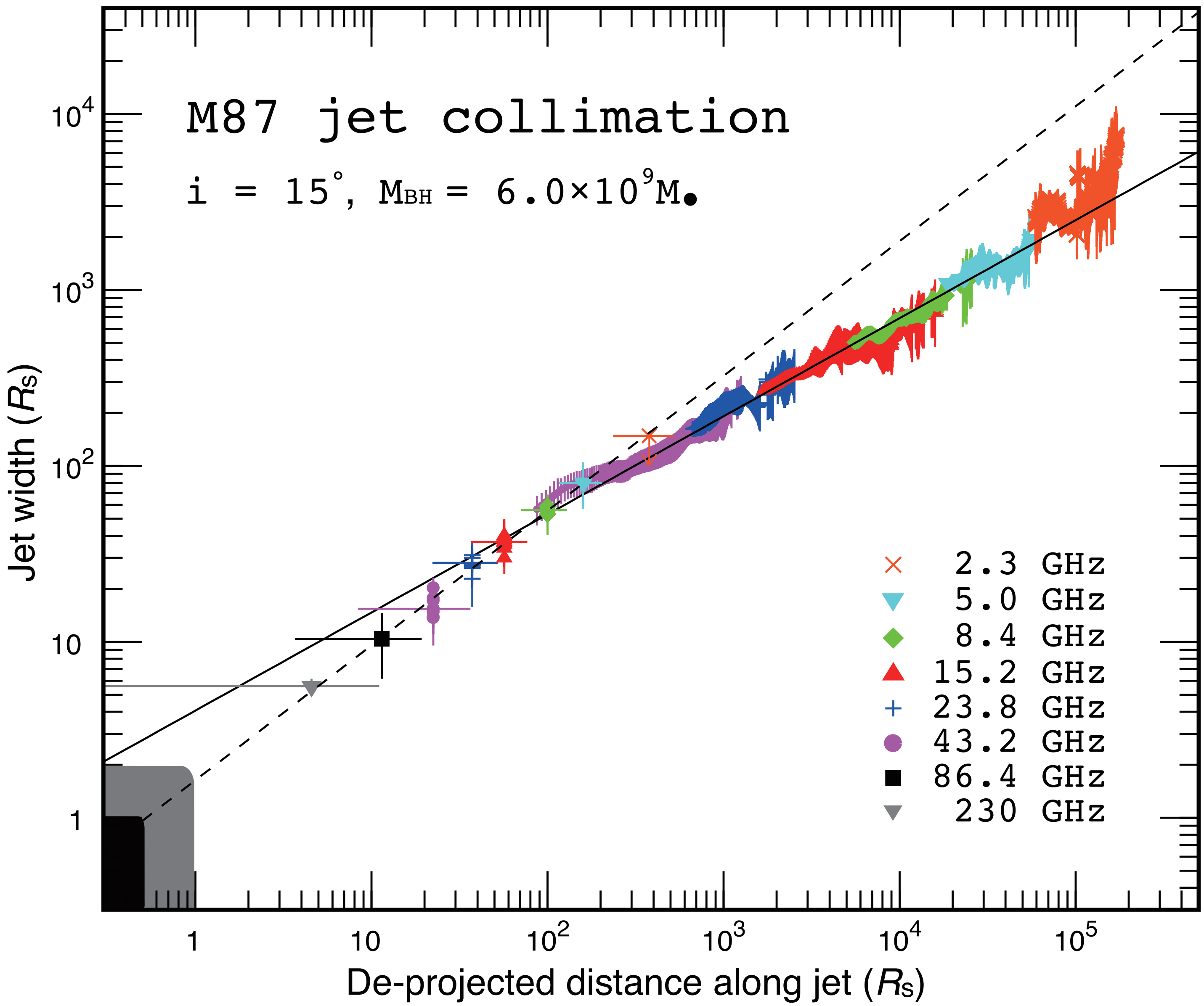

jet from the disk or the black hole?

Transverse profile (Mertens+2016)

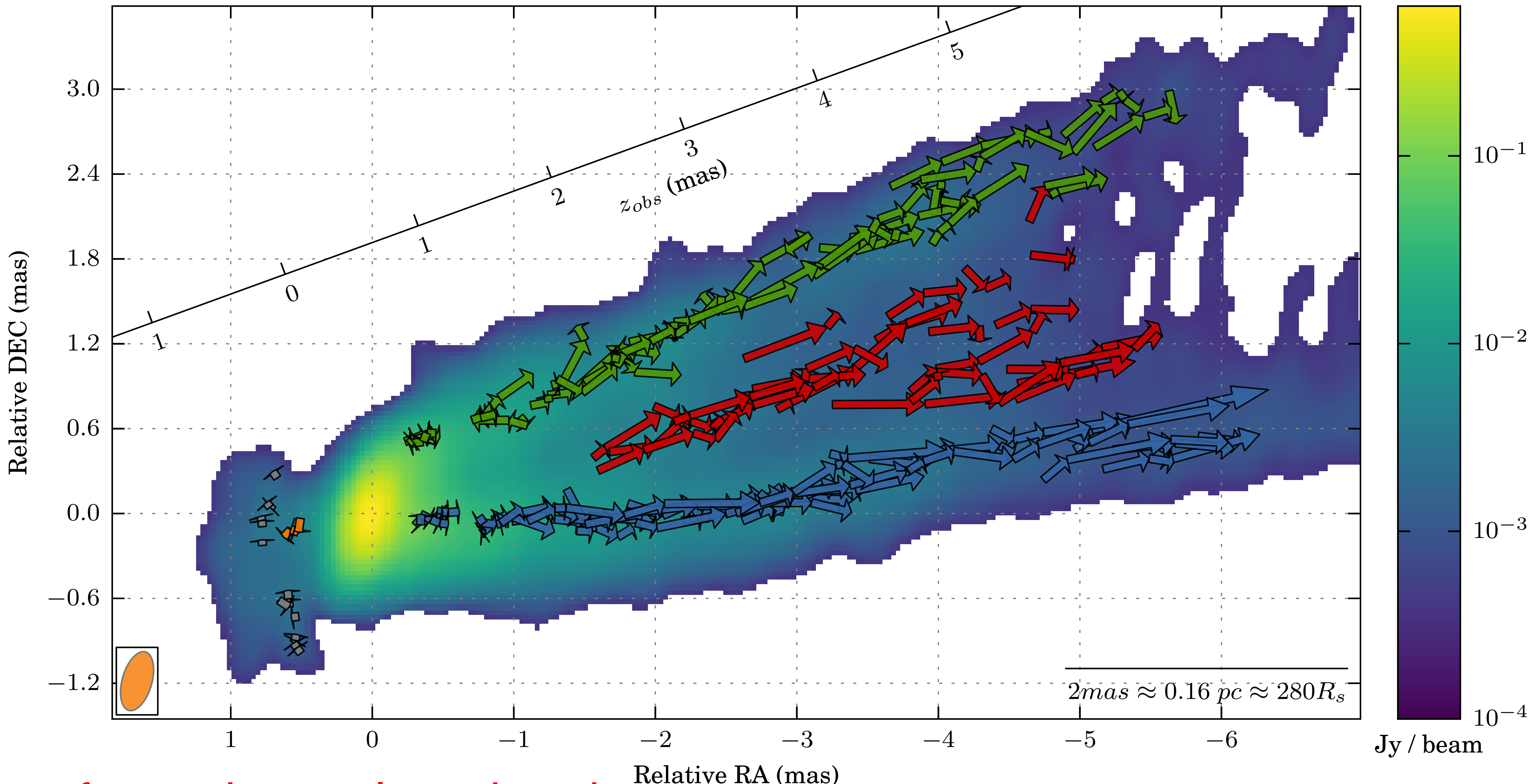

- fast spine – slow sheath
- they manage to observe sheath rotation: the value favors disk-driven (and not BH-driven) jet
- the spine?

(Park+2021)

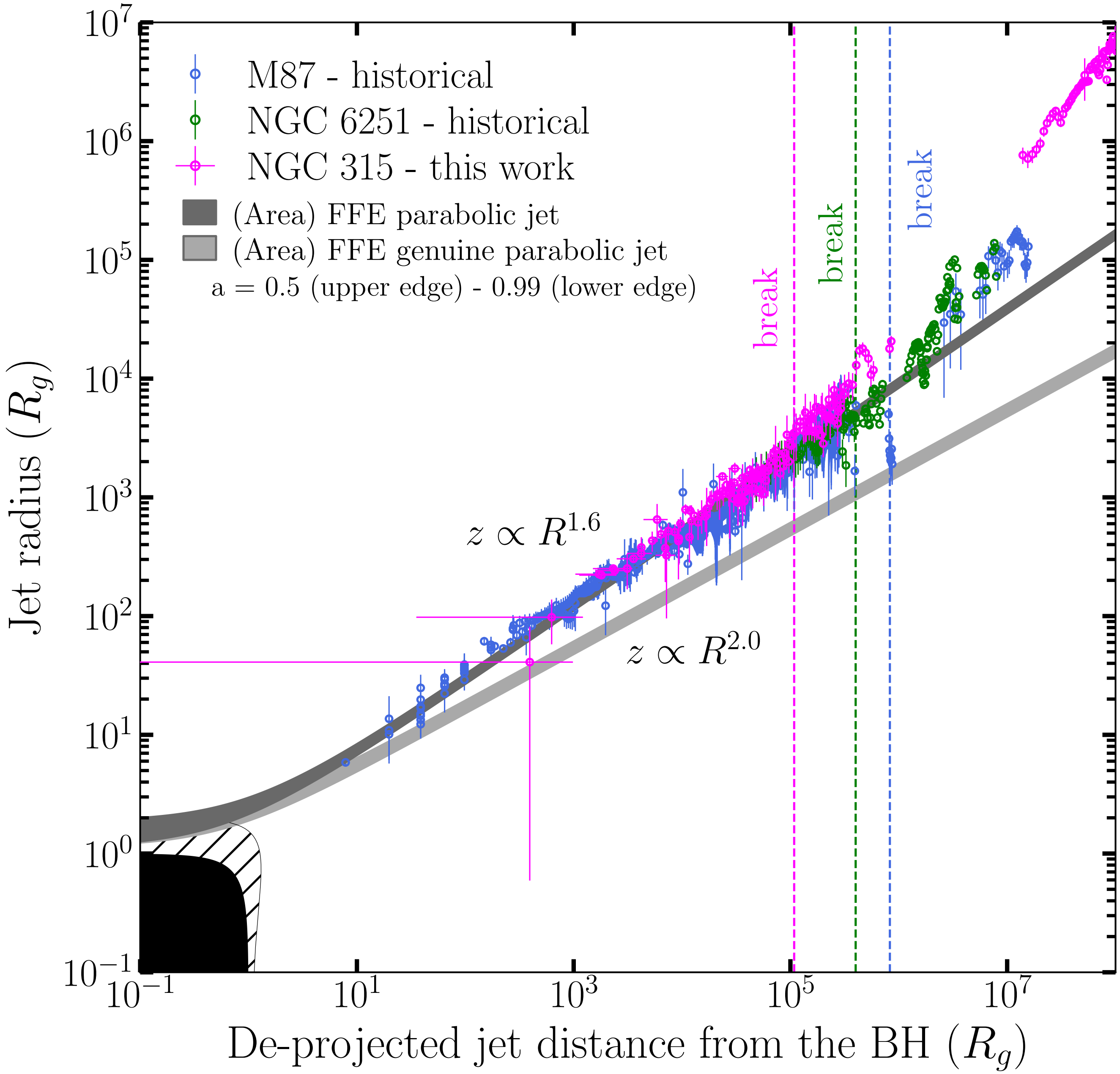

M87 - historical
NGC 6251 - historical
NGC 315 - this work
(Area) FFE parabolic jet
(Area) FFE genuine parabolic jet
a = 0.5 (upper edge) - 0.99 (lower edge)
break
break
break
$z \propto R^{1.6}$
$z \propto R^{2.0}$
Jet radius (R_g)
De-projected jet distance from the BH (R_g)
10^{7}
10^{6}
10^{5}
10^{4}
10^{3}
10^{2}
10^{1}
10^{0}
10^{-1}
10^{-1}
10^{1}
10^{3}
10^{5}
10^{7}

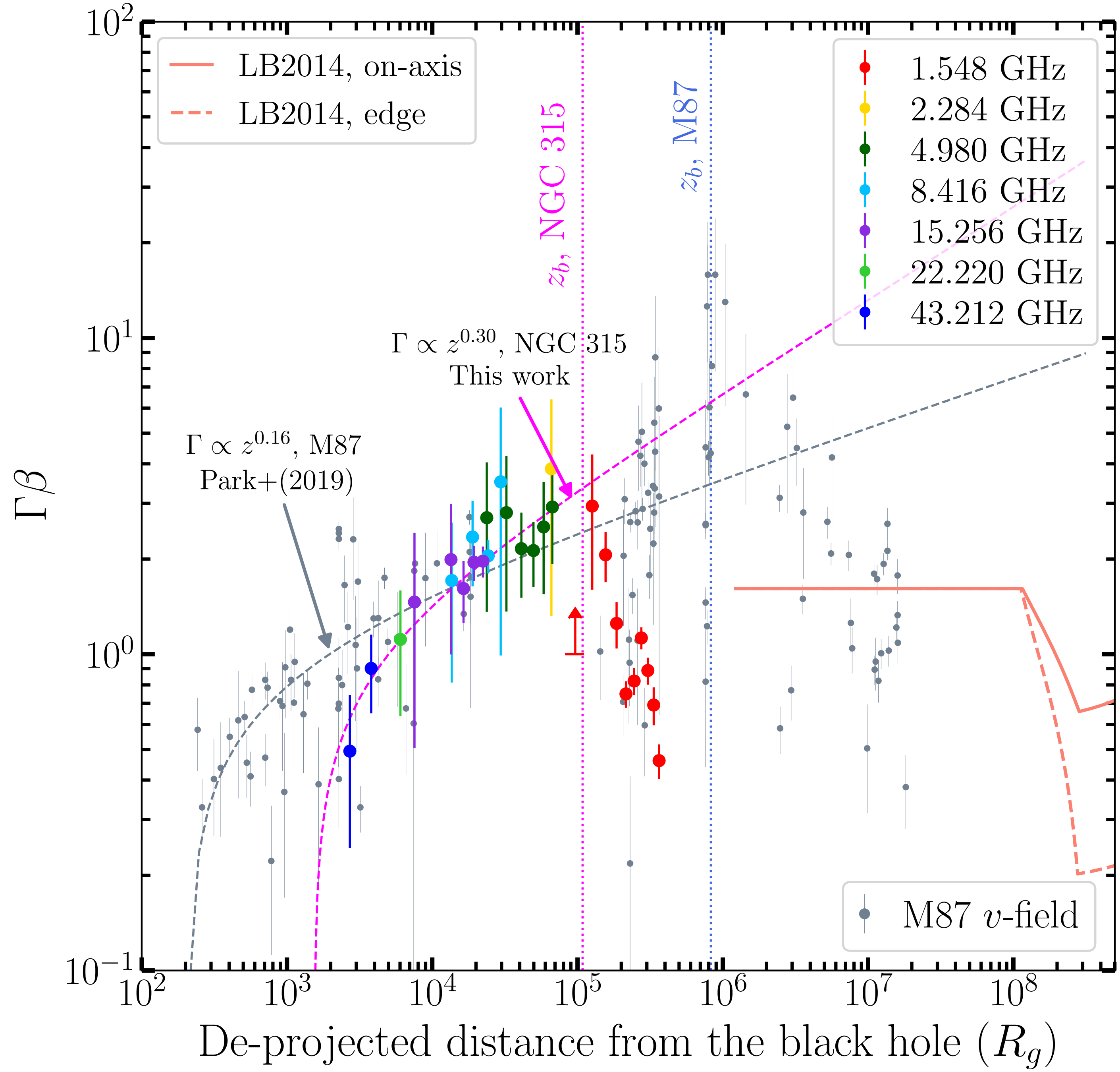

LB2014, on-axis
LB2014, edge
1.548 GHz
2.284 GHz
4.980 GHz
8.416 GHz
15.256 GHz
22.220 GHz
43.212 GHz
z_b, NGC 315
z_b, M87
$\Gamma \propto z^{0.30}$, NGC 315
This work
$\Gamma \propto z^{0.16}$, M87
Park+(2019)
M87 v-field
$\Gamma\beta$
De-projected distance from the black hole (R_g)

X-ray binaries

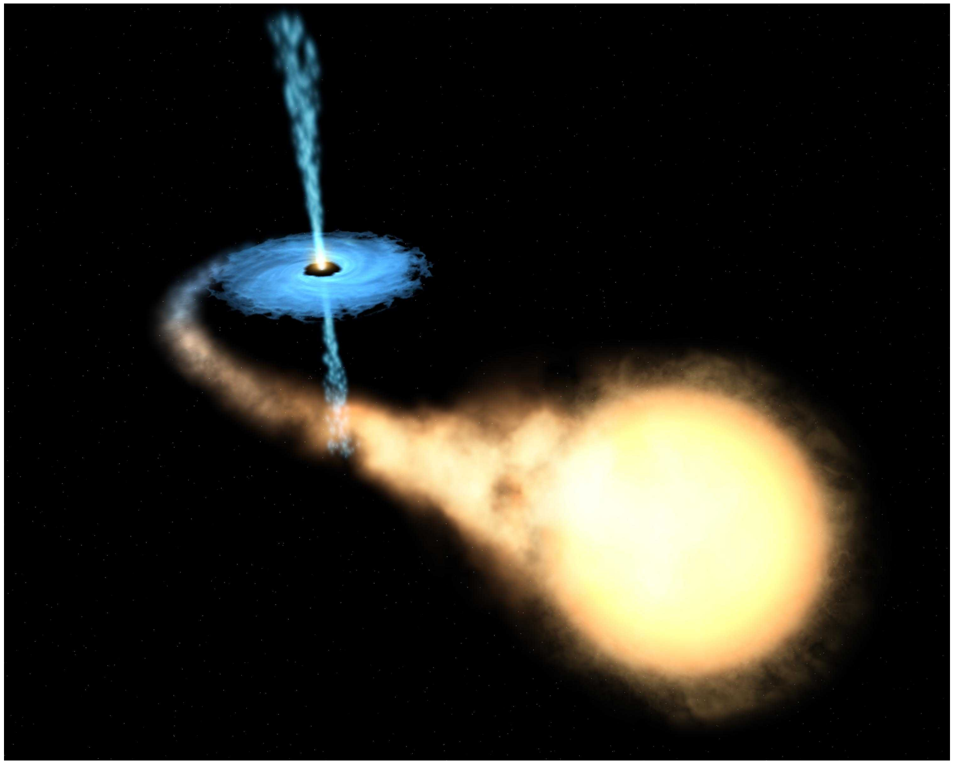

mildly relativistic

γ-ray bursts

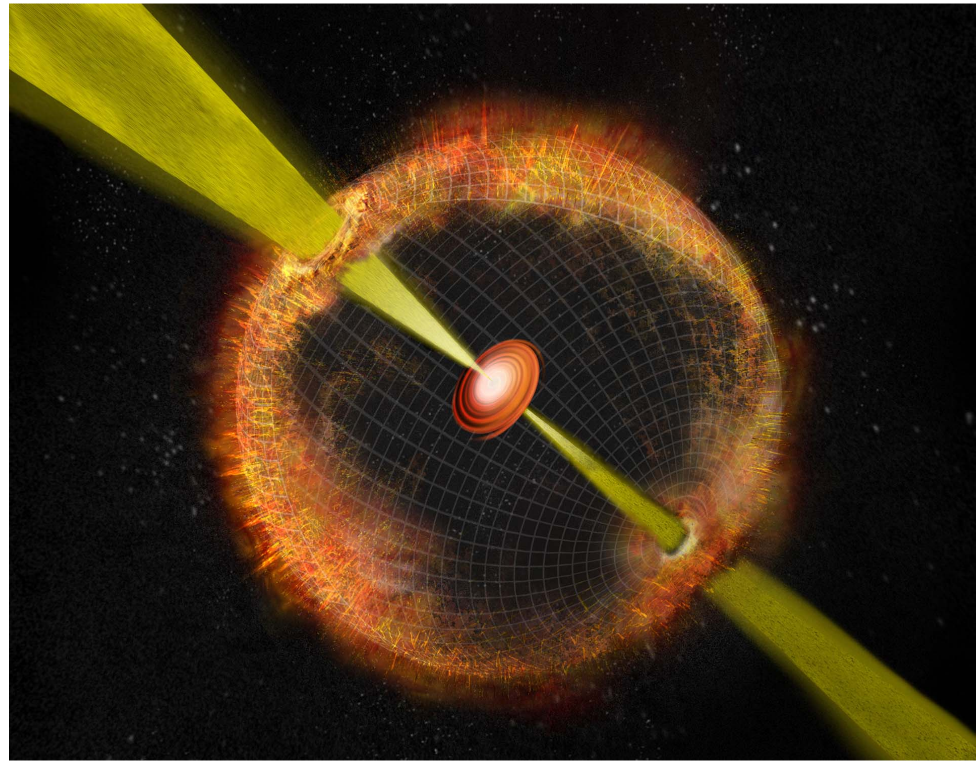

$\gamma =$ a few 100

Basic questions

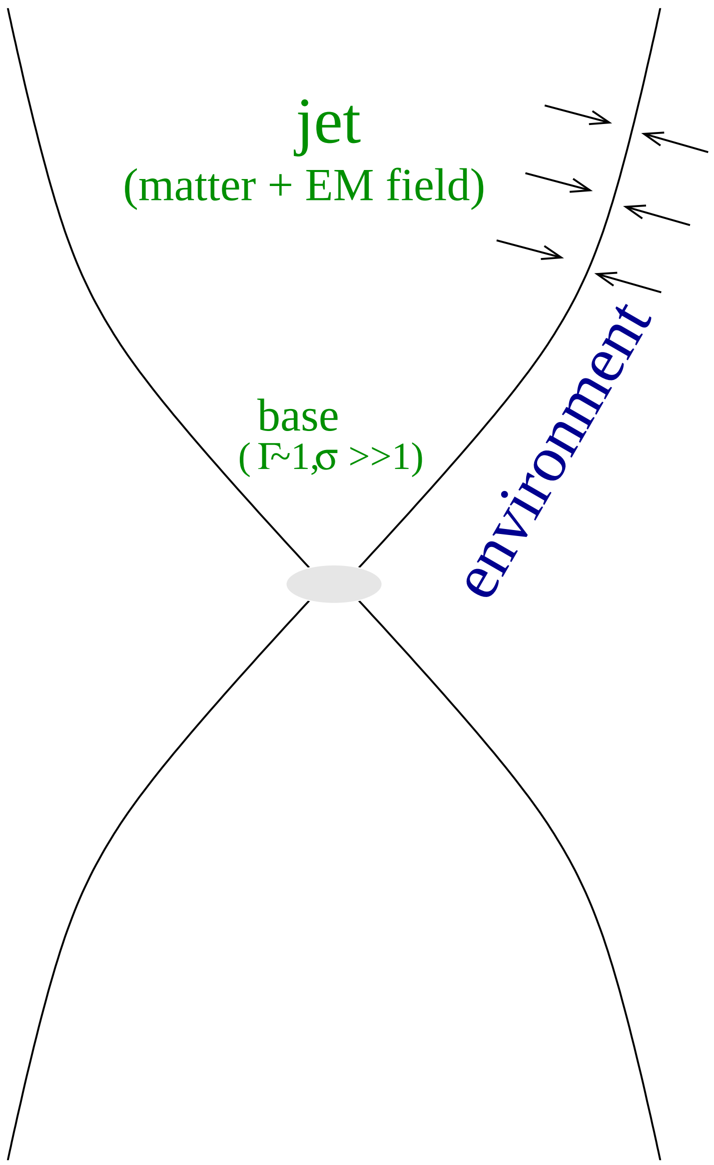

- source of matter/energy?
- bulk acceleration?
- collimation?
- interaction with environment?

Theoretical modeling

- ☞ if energy source = thermal energy:

thermal acceleration is an efficient mechanism

gives terminal speed $\frac{m_p V_\infty^2}{2} \sim k_{\rm B} T_i$ for YSO jets
or terminal Lorentz factors $\gamma_\infty m_p c^2 \sim k_{\rm B} T_i$ for relativistic jets

in both cases needs high initial temperatures T_i to explain the observed motions

- ☞ magnetic acceleration more likely

Polarization

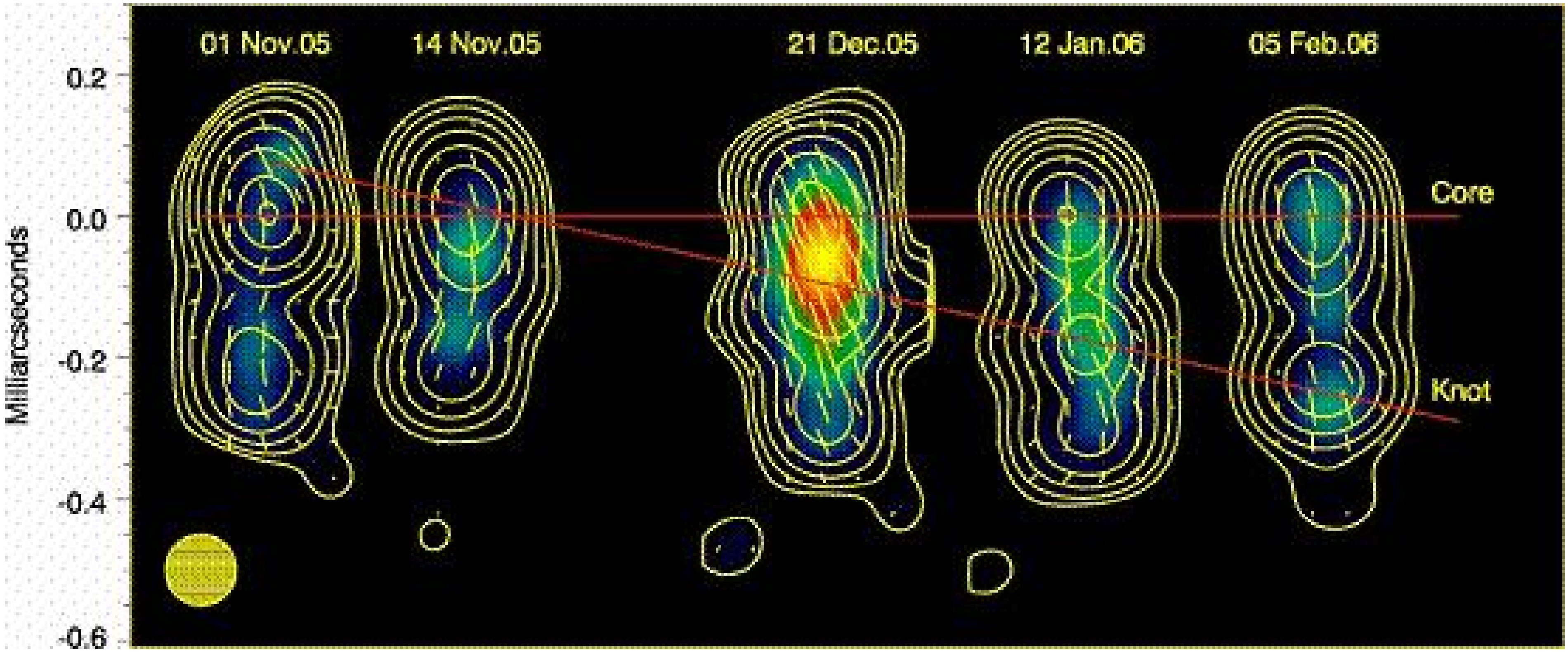

(Marscher et al 2008, Nature)

observed $\boldsymbol{E}_{\mathrm{rad}} \perp \boldsymbol{B}_{\perp \mathrm{los}}$
(modified by Faraday rotation and relativistic effects)

Faraday RM gradients across the jet

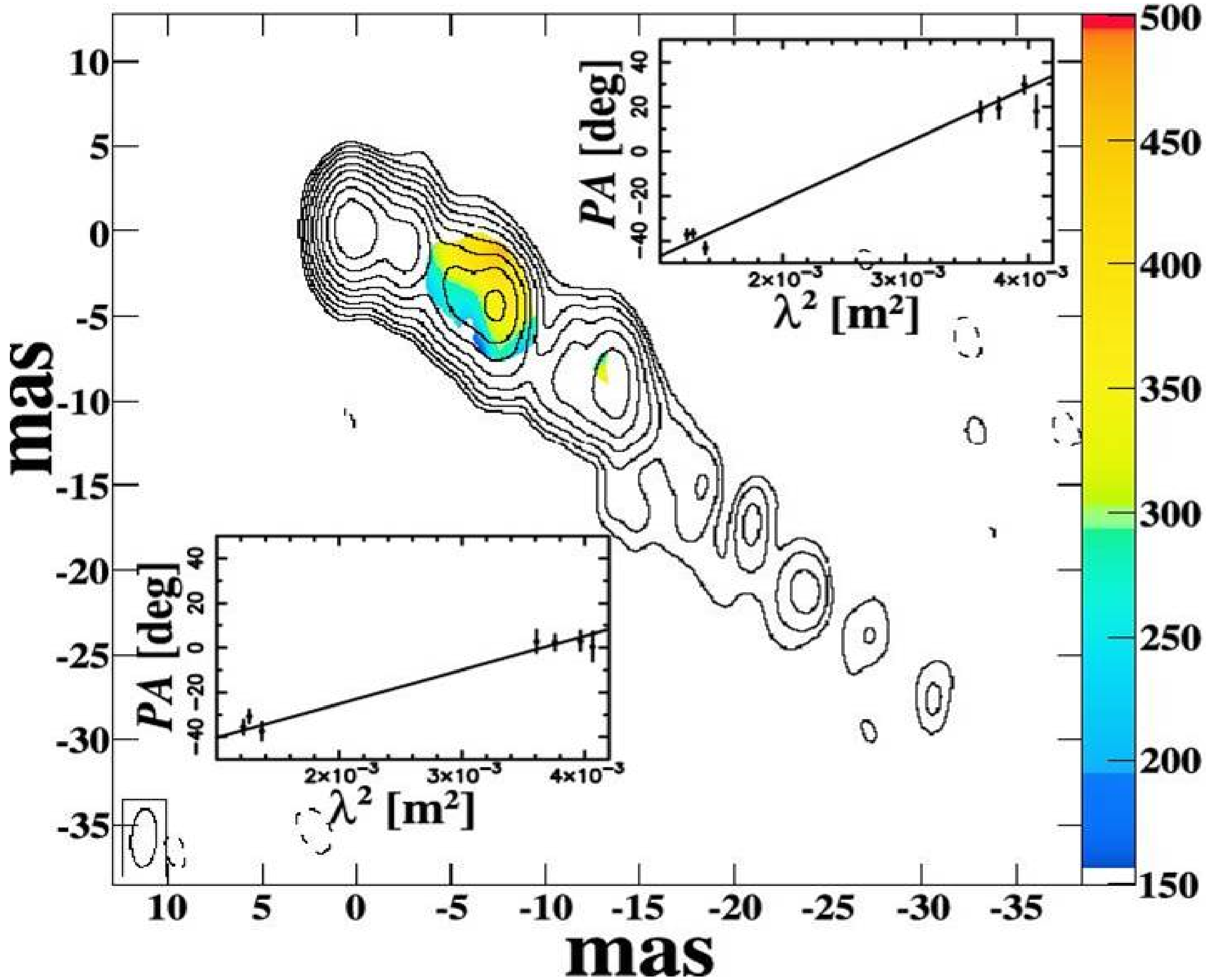

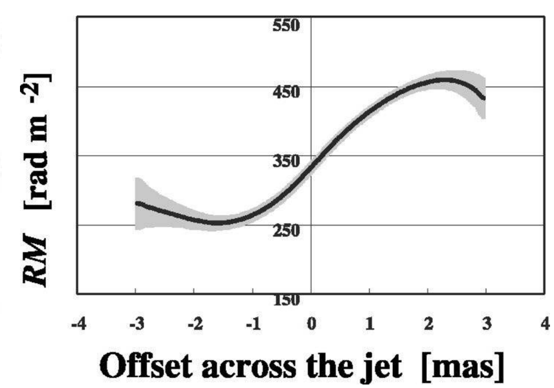

(Asada et al)

helical field surrounding the emitting region (Gabuzda)

Role of magnetic field

- ⋆ extract energy (Poynting flux)
- ⋆ extract angular momentum
- ⋆ transfer energy and angular momentum to matter
- ⋆ explain relatively large-scale acceleration
- ⋆ self-collimation
- ⋆ synchrotron emission
- ⋆ polarization and Faraday RM maps

How MHD acceleration works

A unipolar inductor (Faraday disk)

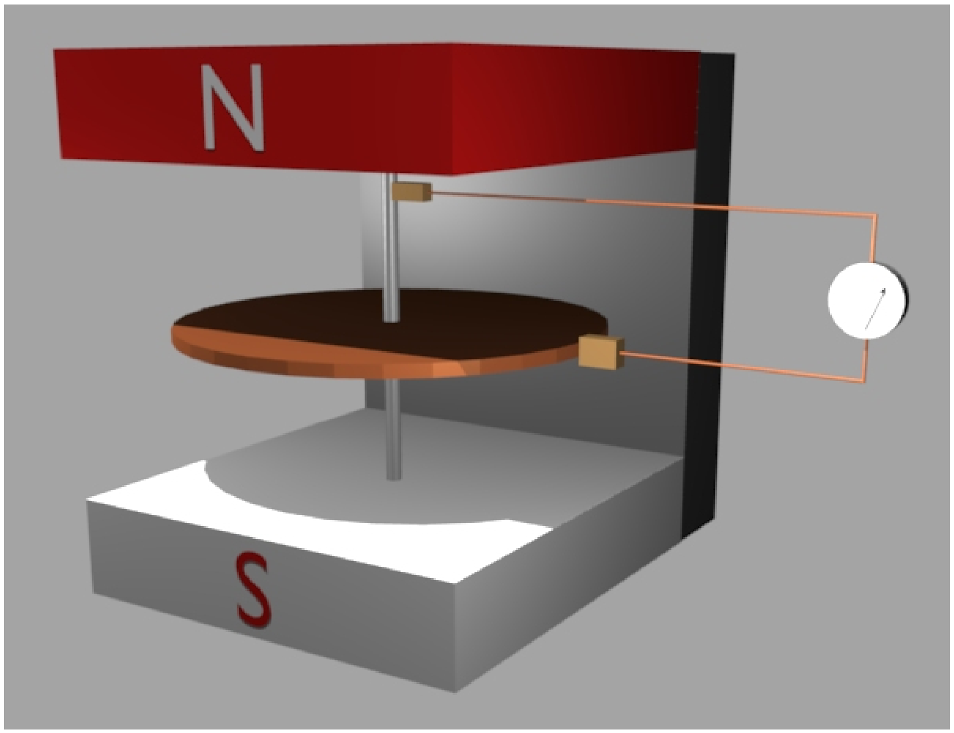

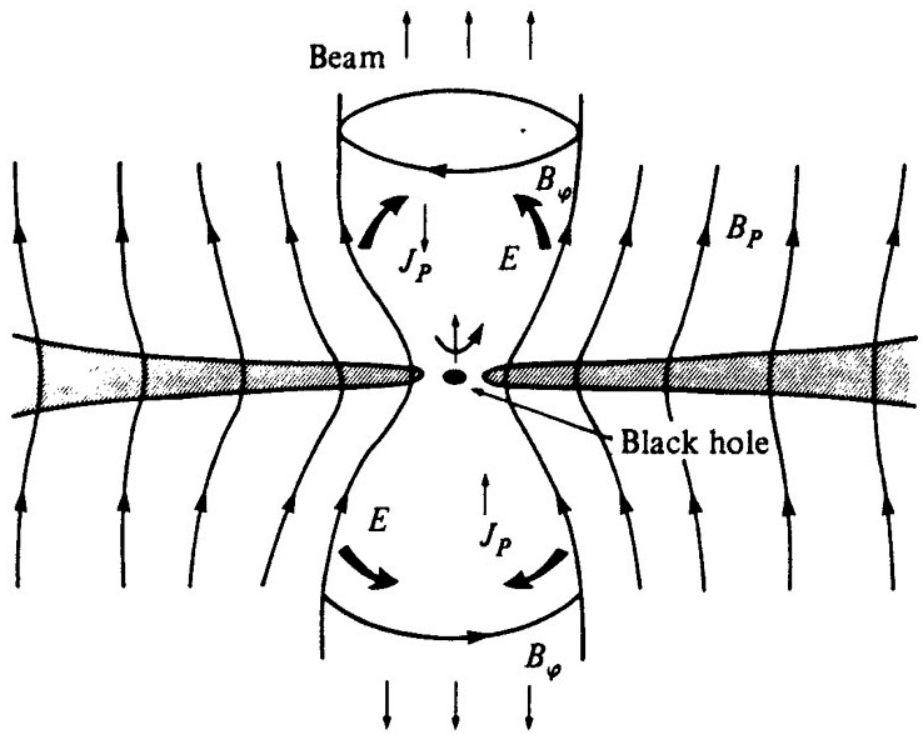

magnetic field + rotation

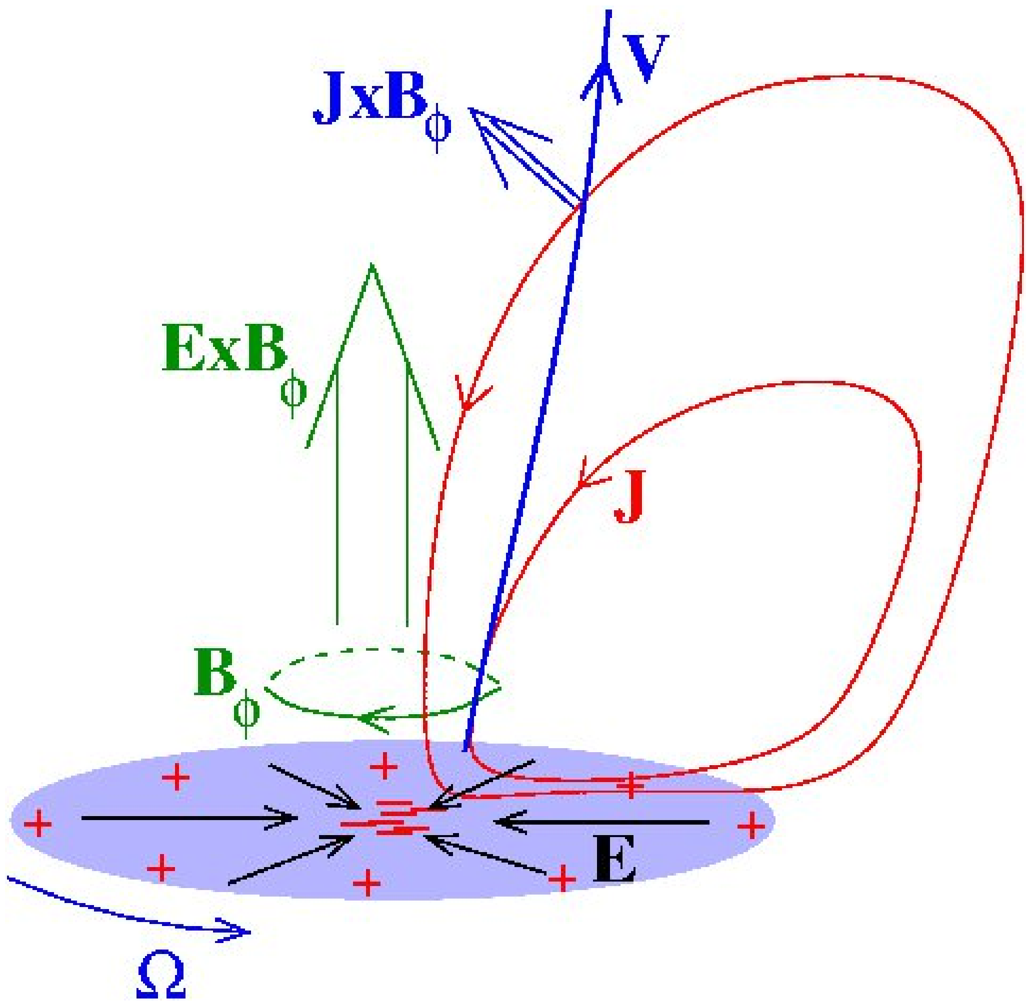

current $\leftrightarrow B_\phi$
Poynting flux $\frac{c}{4\pi}EB_\phi$ is extracted (angular momentum as well)

The Faraday disk could be the rotating accretion disk, or the frame dragging if energy is extracted from the ergosphere of a rotating black hole (Blandford & Znajek mechanism)

The ideal MHD equations

Maxwell:

$$\boldsymbol{\nabla}\cdot\boldsymbol{B}=0=\boldsymbol{\nabla}\times\boldsymbol{E}+\frac{\partial\boldsymbol{B}}{c\partial t}\,,\,\boldsymbol{\nabla}\times\boldsymbol{B}=\frac{\partial\boldsymbol{E}}{c\partial t}+\frac{4\pi}{c}\boldsymbol{J}\,,\,\boldsymbol{\nabla}\cdot\boldsymbol{E}=\frac{4\pi}{c}J^0$$

Ohm: $\boldsymbol{E}=-\frac{\boldsymbol{V}}{c}\times\boldsymbol{B}$

mass conservation (continuity):

$$\frac{d(\gamma\rho_0)}{dt}+\gamma\rho_0\boldsymbol{\nabla}\cdot\boldsymbol{V}=0\,,\quad \text{where}\quad \frac{d}{dt}=\frac{\partial}{\partial t}+\boldsymbol{V}\cdot\boldsymbol{\nabla}$$

energy $U_\mu T^{\mu\nu}_{,\nu}=0$ (or specific entropy conservation, or first law for thermodynamics):

$$\frac{d\left(P/\rho_0^\Gamma\right)}{dt}=0$$

momentum $T^{\nu i}_{,\nu}=0$: $\gamma\rho_o\frac{d\left(\xi\gamma\boldsymbol{V}\right)}{dt}=-\boldsymbol{\nabla}P+\frac{J^0\boldsymbol{E}+\boldsymbol{J}\times\boldsymbol{B}}{c}$

magnetic acceleration

- simplified momentum equation along the flow

$$\gamma\rho_0\frac{d(\gamma V)}{dt} = -\frac{B_\phi}{4\pi\varpi}\frac{\partial(\varpi B_\phi)}{\partial \ell} \qquad = \boldsymbol{J}\times\boldsymbol{B} \text{ force}$$

(ϖ= cylindrical distance, ℓ= arclength along flow)

- simplified Ferraro's law (ignore V_ϕ – small compared to $\varpi\Omega$)

$$V_\phi = \varpi\Omega + V B_\phi/B_p \quad \Leftrightarrow \quad B_\phi \approx -\frac{\varpi\Omega B_p}{V} \quad \text{“Parker spiral”}$$

- combine the two, use the mass-to-magnetic flux $\Psi_A = \dfrac{4\pi\gamma\rho_0 V}{B_p}$

(constant due to flux-freezing)

$$m\frac{d(\gamma V)}{dt} = -\frac{\partial}{\partial\ell}\left(\frac{S}{V}\right), \quad m = \frac{\Psi_A}{A\Omega^2}, \quad S = \frac{\varpi^2 B_p}{A}$$

(A is the magnetic flux – integral)

toy model

$$m\frac{d(\gamma V)}{dt} = -\frac{\partial}{\partial \ell}\left(\frac{S}{V}\right)$$

motion of a mass $m = \dfrac{\Psi_A}{A\Omega^2}$ in a velocity-dependent potential $\dfrac{S}{V}$

corresponding energy integral = Bernoulli $\gamma mc^2 + \dfrac{S}{V} = E$

The equation of particle motion can be written as a de-Laval nozzle equation

$$\frac{dV}{d\ell} = \frac{\dfrac{dS}{d\ell}}{E - \gamma^3 mc^2}$$

bunching function $S = \varpi^2 B_p / A$

using the definition of A, $$S = \frac{2\pi\varpi^2 B_p}{\displaystyle\int \boldsymbol{B}_p \cdot d\boldsymbol{a}}$$

thus S measures the ratio of the local over the mean poloidal magnetic field

it measures how bunched are the fieldlines at a given point

its variation along the flow measures the expansion of the flow,

$$S \propto \frac{\varpi}{\underbrace{B_p\, 2\pi\varpi\delta\ell_\perp}_{\delta A}\, \delta\ell_\perp} \propto \frac{\varpi}{\delta\ell_\perp}$$

if $\delta\ell_\perp/\varpi$ increases, S decreases if $\delta\ell_\perp/\varpi$ decreases, S increases

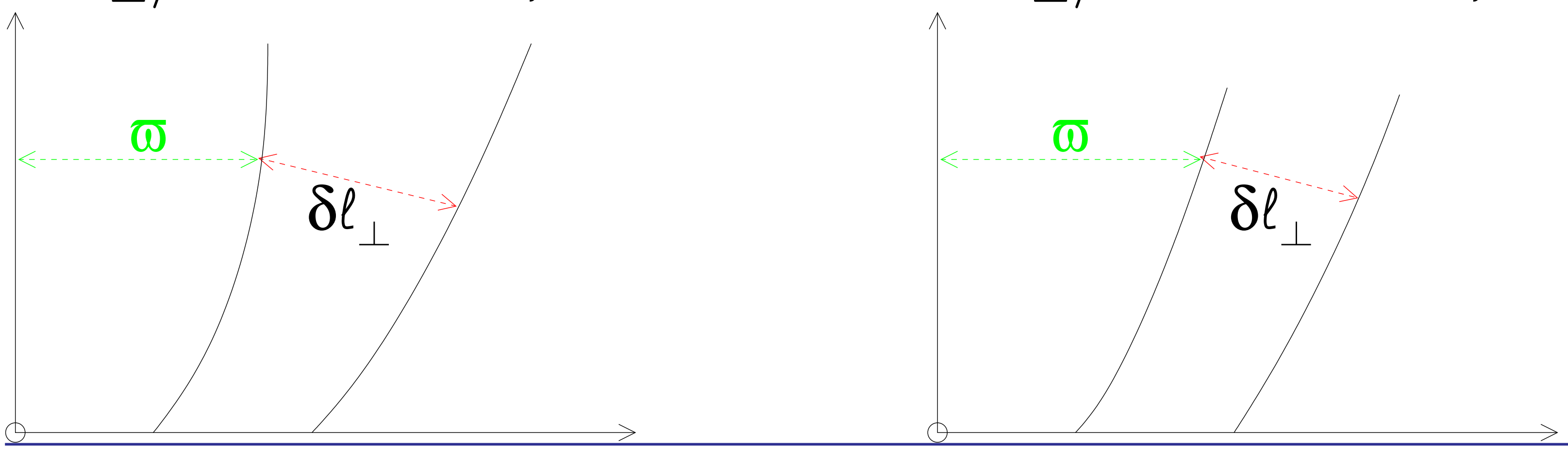

Vlahakis+2000 nonrelativistic solution

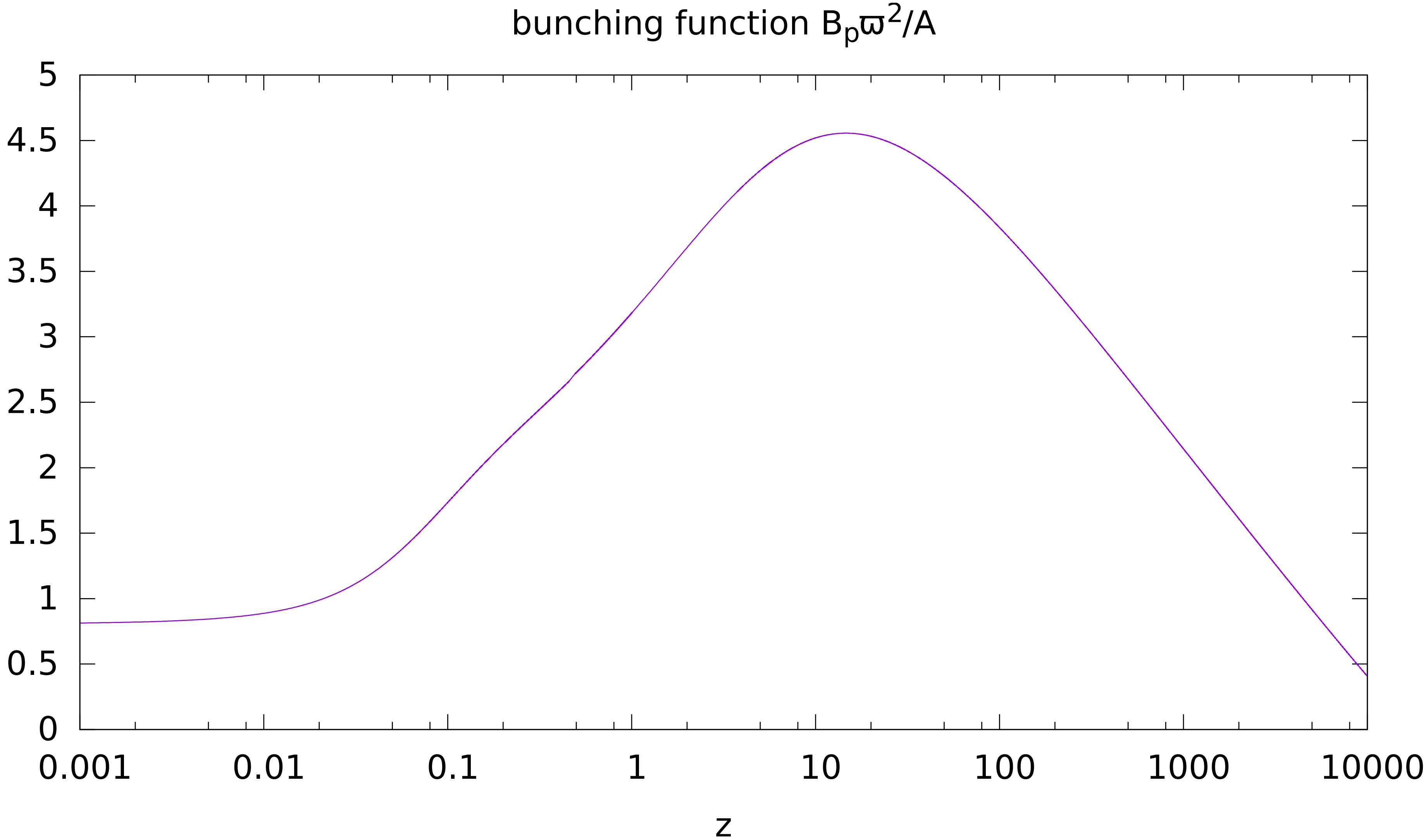

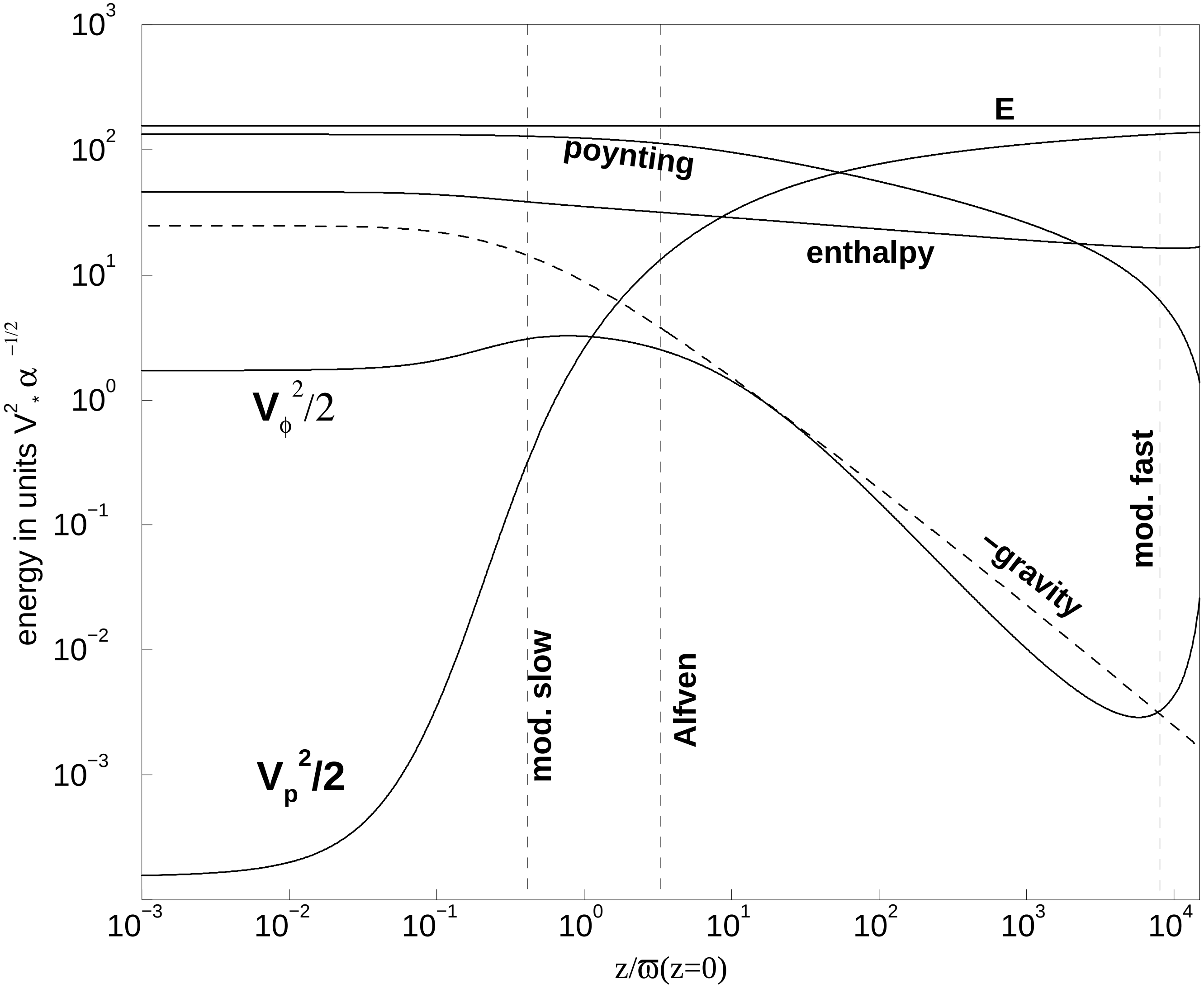

E
poynting
enthalpy
$V_\phi^2/2$
$V_p^2/2$
mod. slow
Alfven
−gravity
mod. fast
energy in units $V_*^2\,\alpha^{-1/2}$
$z/\varpi(z=0)$

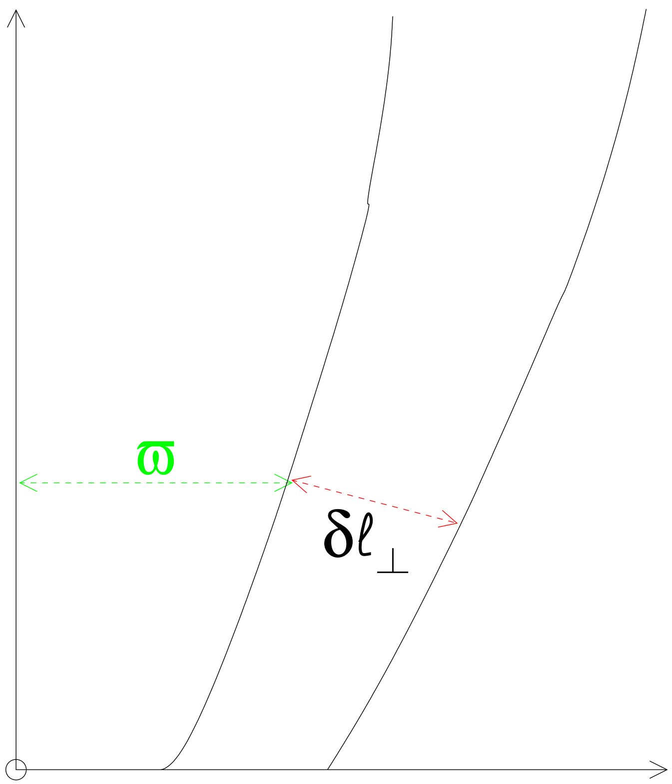

first S increases then decreases (differential collimation)

$S_\infty \sim 1$ so the Bernoulli integral gives the value of V_∞

higher $S_{\rm max}$ $\rightarrow$ higher acceleration efficiency

in V00 $S_{\rm max} \approx 4.5$ and acceleration efficiency $\gtrsim 90\%$

Vlahakis & Königl 2003, 2004 relativistic solutions

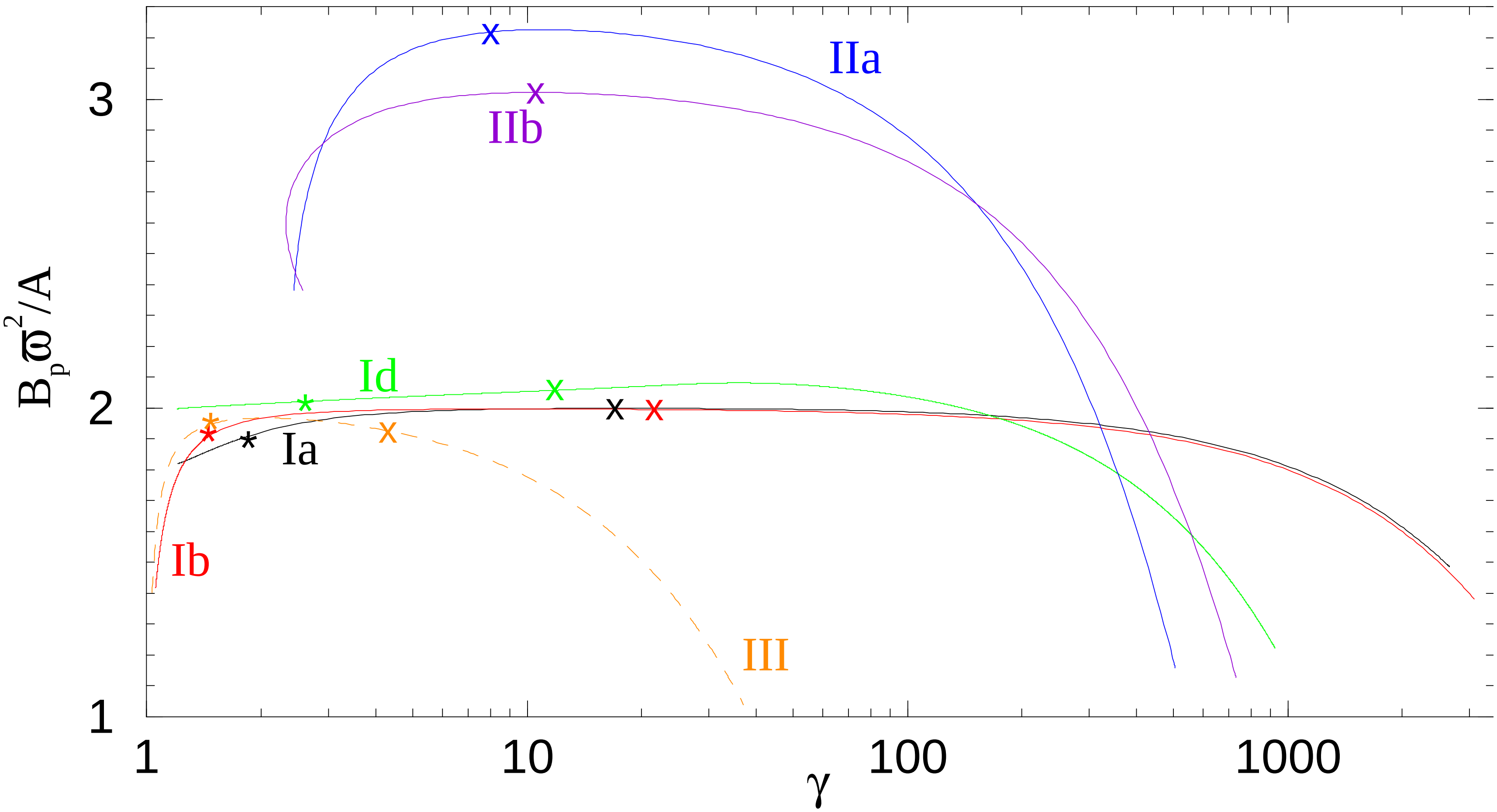

acceleration efficiency $\gtrsim 50\%$

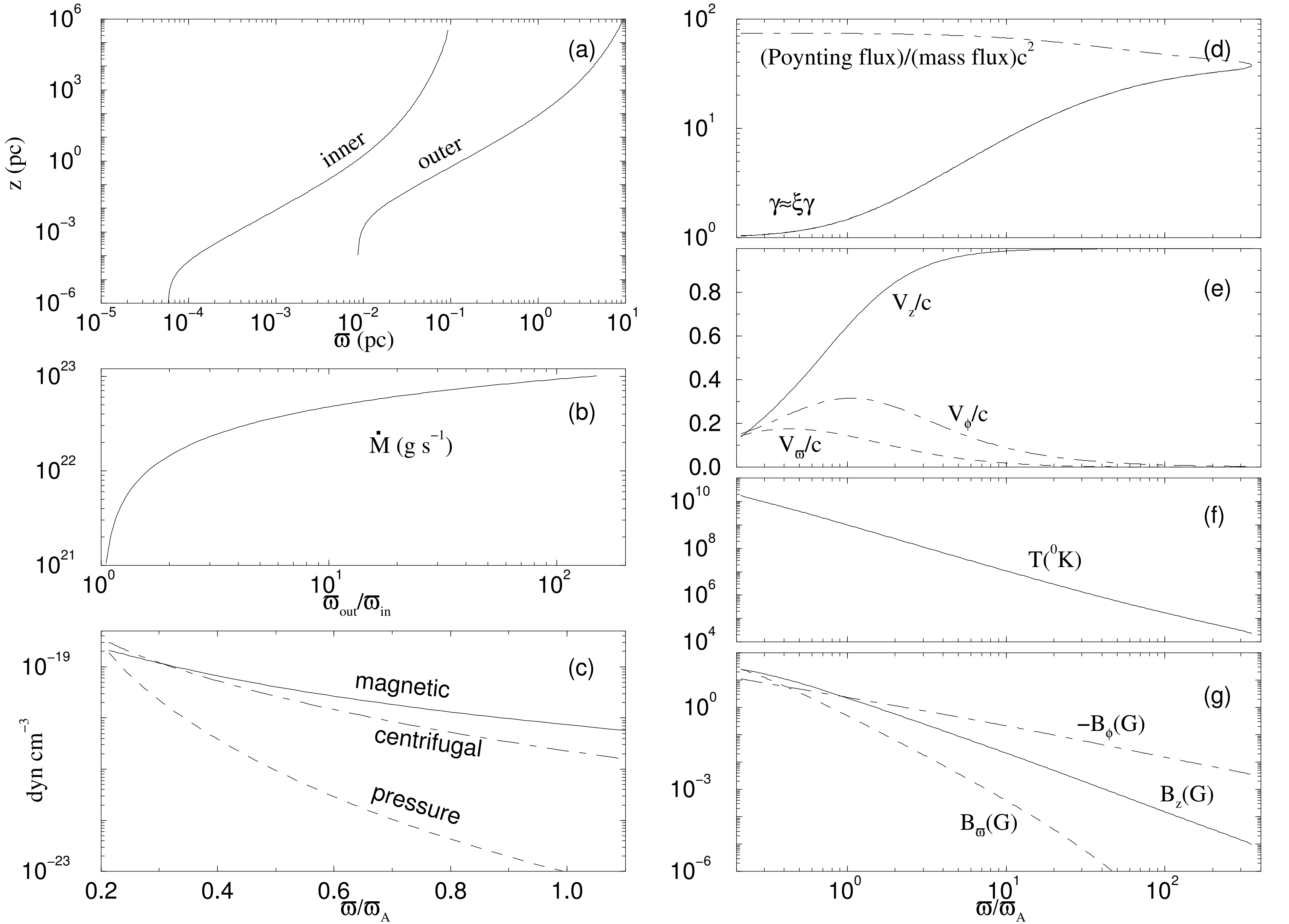

(a)
inner
outer
z (pc)
ϖ (pc)
(b)
Ṁ (g s^{-1})
ϖ$_{out}$/ϖ$_{in}$
(c)
magnetic
centrifugal
pressure
dyn cm^{-3}
ϖ/ϖ$_A$
(d)
(Poynting flux)/(mass flux)c^2
γ≈ξγ
(e)
V$_z$/c
V$_\phi$/c
V$_ϖ$/c
(f)
T(^{0}K)
(g)
−B$_\phi$(G)
B$_z$(G)
B$_ϖ$(G)
ϖ/ϖ$_A$

Simulations of special relativistic jets (e.g. Komissarov+2009)

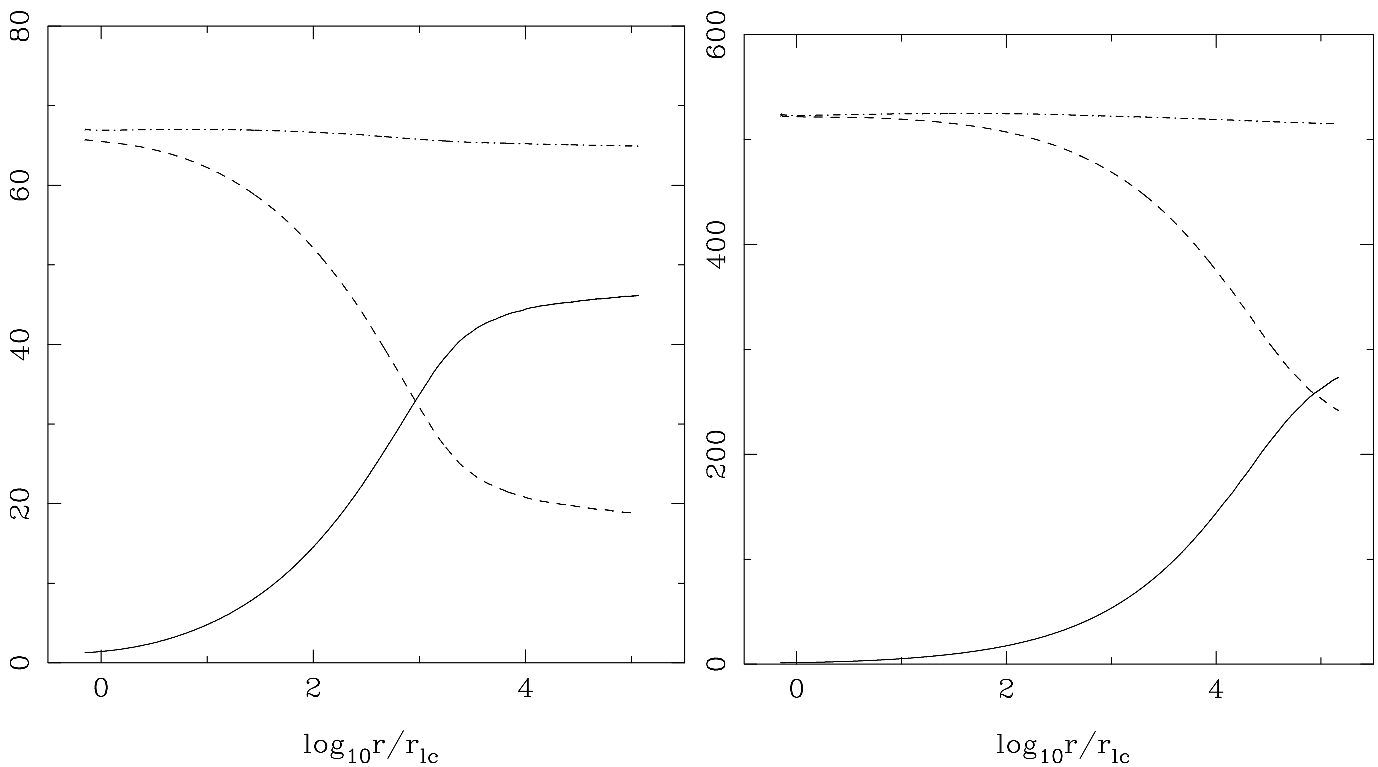

energy flux ratios:

$$\gamma = \frac{\text{kinetic}}{\text{rest mass}}$$

$$\gamma\sigma = \frac{\text{Poynting}}{\text{rest mass}}$$

$$(\sigma = \frac{\text{Poynting}}{\text{kinetic}})$$

$$\mu = \gamma + \gamma\sigma$$

γ (increasing),

$\gamma\sigma$ (decreasing),

and μ (constant)

efficiency $> 50\%$

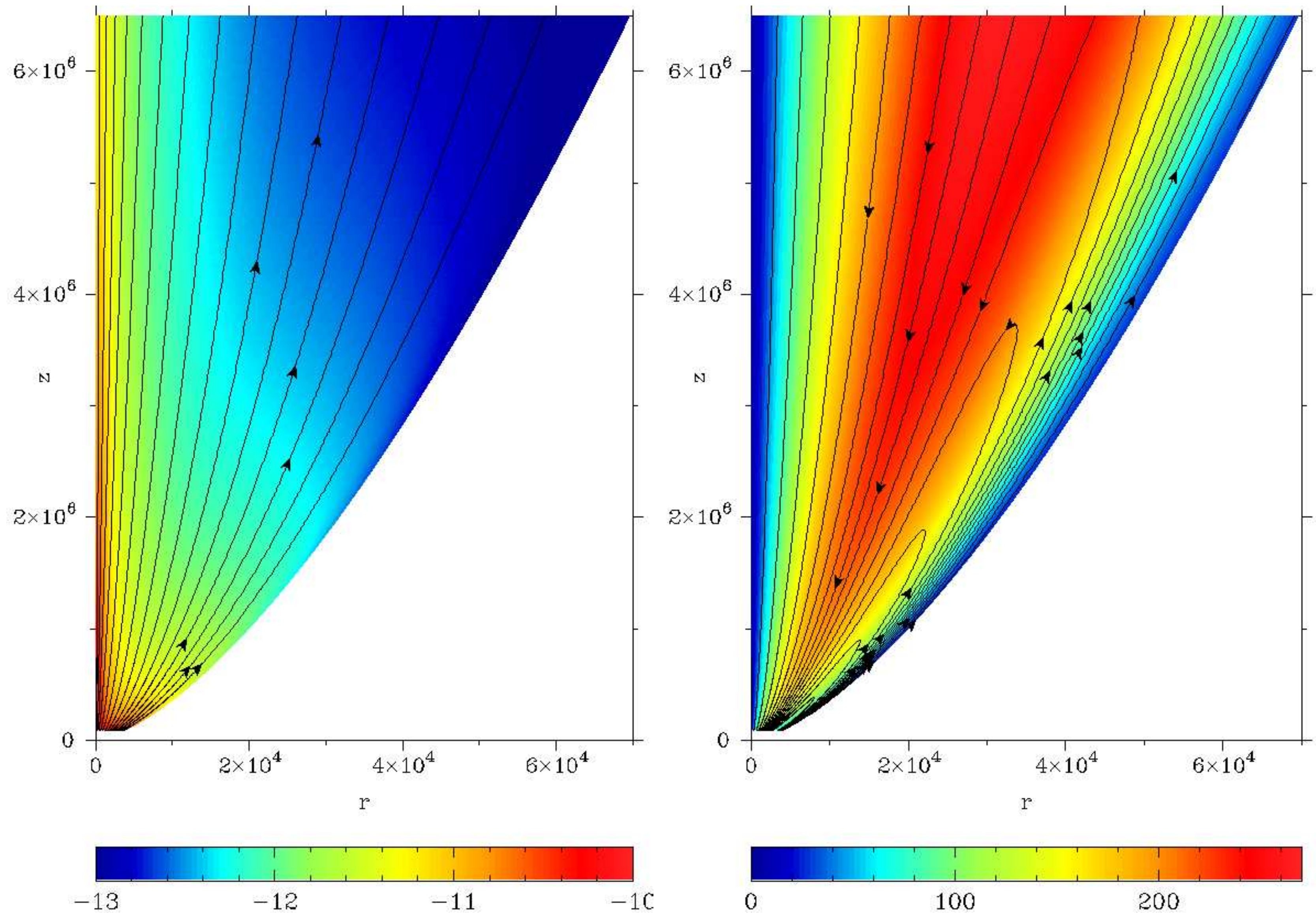

left: density/field lines, right: Lorentz factor/current lines (jet shape $z \propto r^{1.5}$)

Even in general relativistic MHD jet simulations (Chatterjee+2019 - review Mizuno 2022)

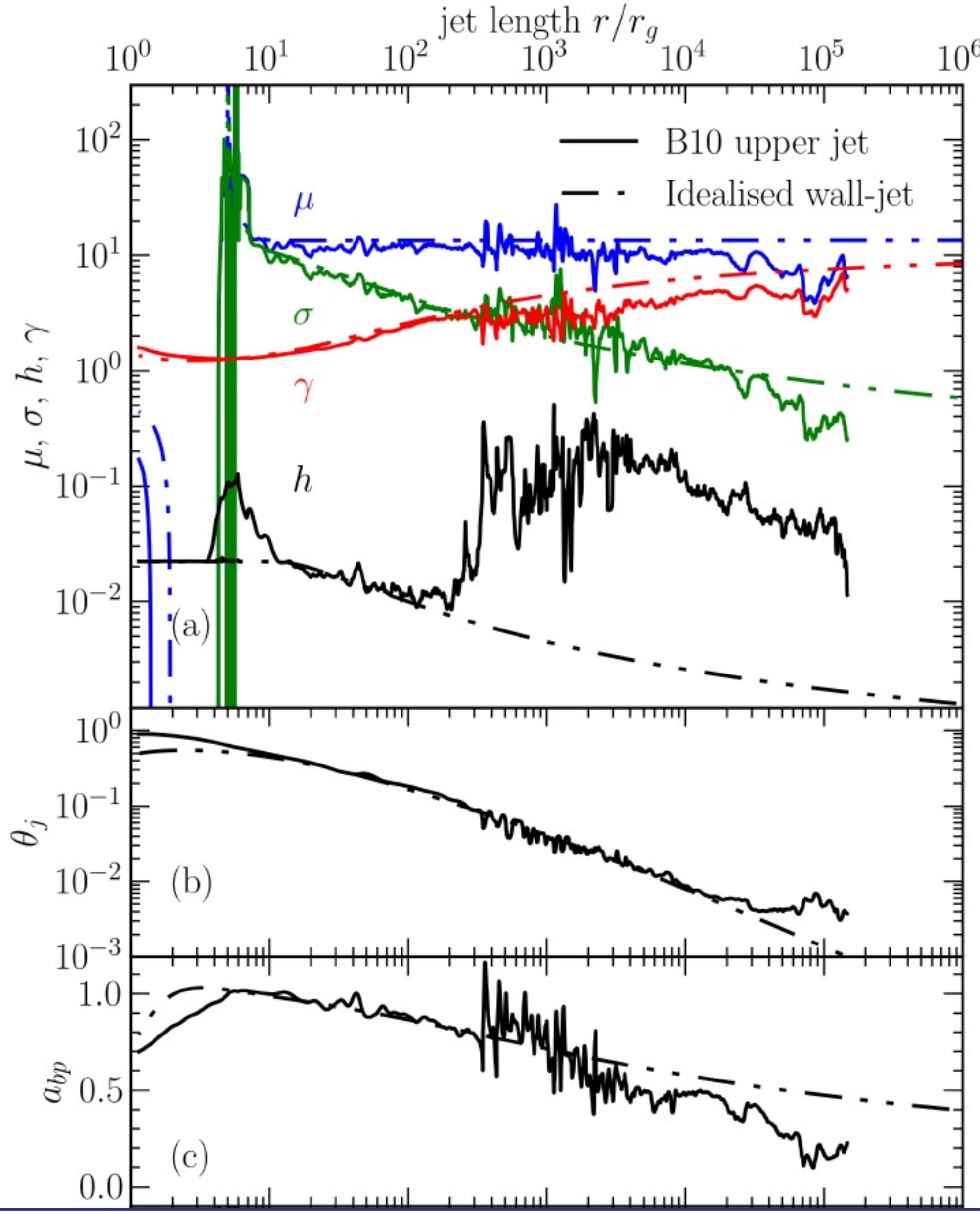

Basic questions: collimation

hoop-stress:

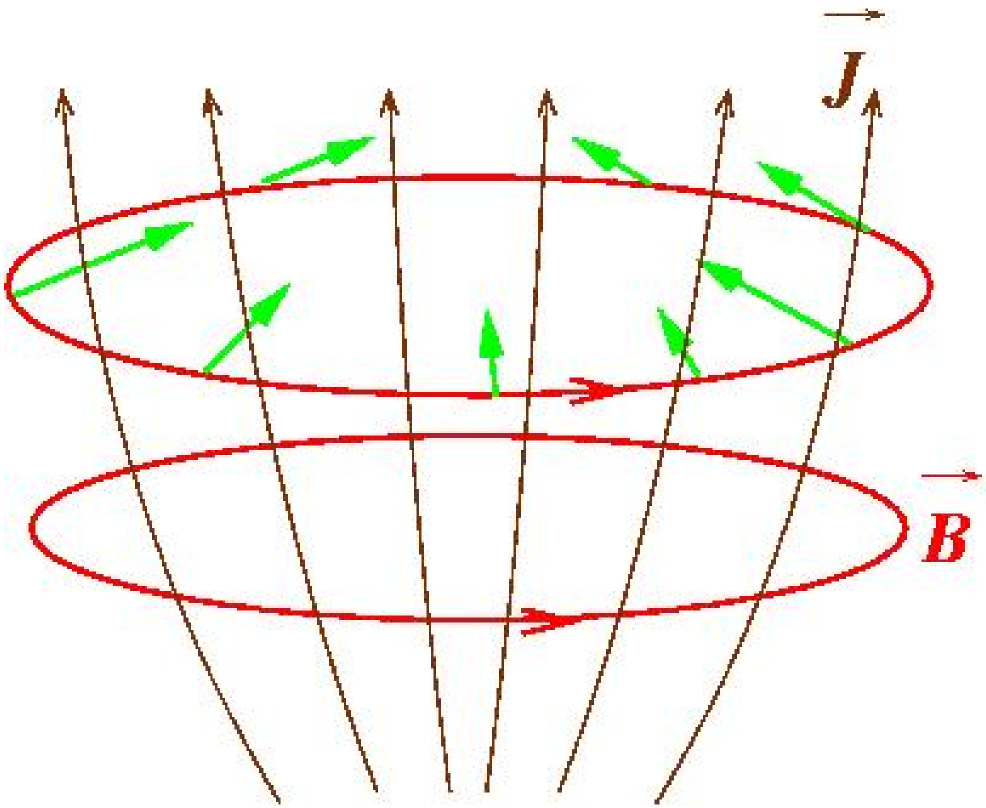

+ electric force

degree of collimation ?

Role of environment?

☞ transfield component of the momentum equation for relativistic jets simplifies to $\mathcal{R} \approx \gamma^2 \varpi$

since $\mathcal{R}^{-1} \approx -\frac{d^2\varpi}{dz^2} \approx \frac{\varpi}{z^2}$ it gives power-law $\gamma \approx z/\varpi$
(for parabolic shapes $z \propto \varpi^a$, γ is a power of ϖ)

☞ role of external pressure

$p_{\rm ext} = B_{\rm co}^2/8\pi \simeq (B^{\hat\phi})^2/8\pi\gamma^2 \propto 1/\varpi^2\gamma^2$

- if the pressure drops slower than z^{-2} then
  - ⋆ shape more collimated than $z \propto \varpi^2$
  - ⋆ linear acceleration $\gamma \propto \varpi$
- if the pressure drops as z^{-2} then
  - ⋆ parabolic shape $z \propto \varpi^a$ with $1 < a \leq 2$
  - ⋆ first $\gamma \propto \varpi$ and then power-law acceleration $\gamma \sim z/\varpi \propto \varpi^{a-1}$
- if pressure drops faster than z^{-2} then
  - ⋆ conical shape
  - ⋆ linear acceleration $\gamma \propto \varpi$ (small efficiency)

Basic questions

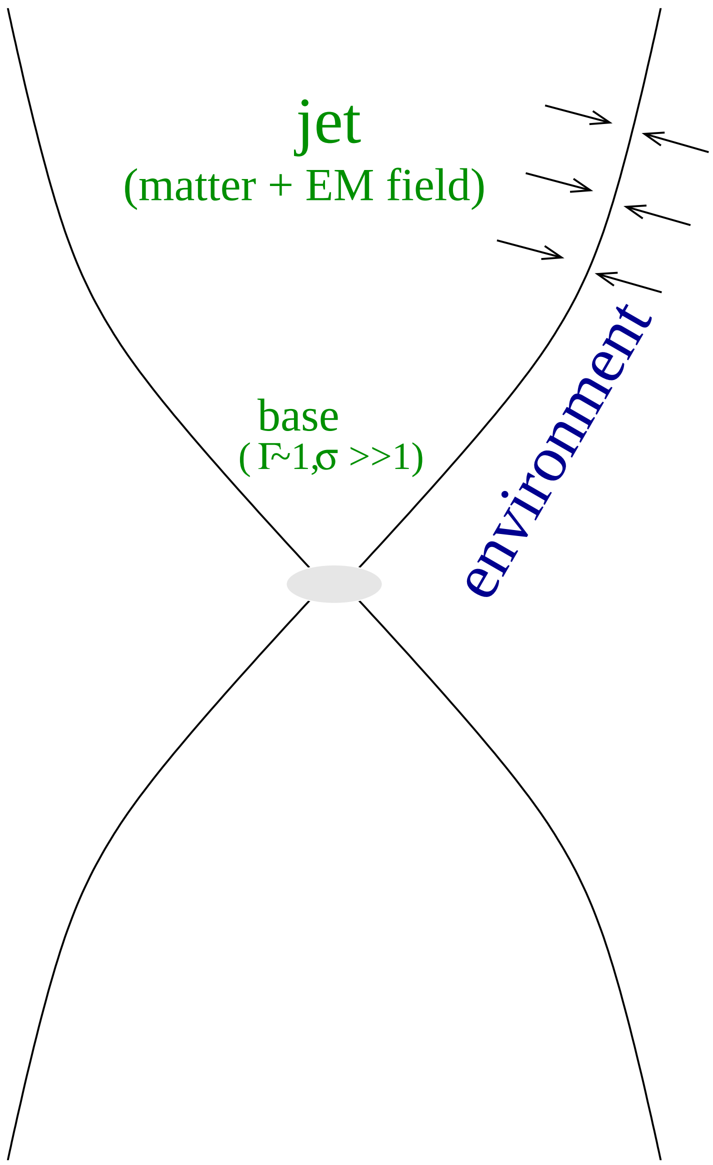

- source of matter/energy?
disk or central object, rotation+magnetic field

- bulk acceleration ✓

- collimation ✓

- interaction with environment?
$P_{\rm ext}$ is important especially in relativistic jets

2nd level of understanding

- ☞ distribution of B in the source? (advection vs diffusion, instabilities in disks?)

- ☞ details of jet physics near rotating black holes (pair creation in stagnation surface) – energy extraction from the black hole?

- ☞ nonthermal radiation – particle acceleration

  shocks or reconnection ? connection with instabilities ?

- ☞ polarization maps and comparison with observations

- ☞ detailed study of the interaction with environment (Riemann problem – shock and rarefaction waves)

- ☞ jet stability (Kelvin-Helmholtz? current driven?)

Magnetohydrodynamics

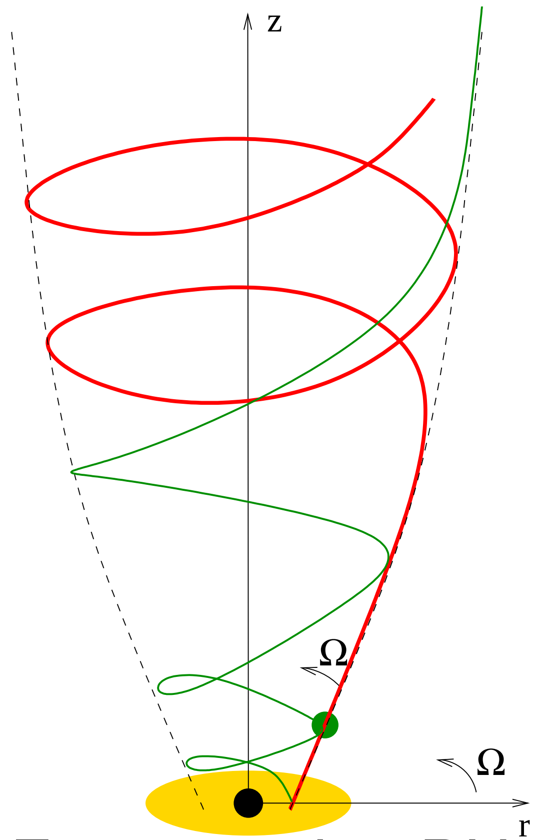

- successfully explain the main characteristics

- At small distances $V_\phi \gg V_p$, $|B_\phi| \ll B_p$. At large distances $V_\phi \ll V_p$, $|B_\phi| \gg B_p$.

- From Ferraro's law $V_\phi = \varpi\Omega + V B_\phi / B_p$, where Ω integral of motion = rotation at base, we get $-B_\phi/B_p \approx \varpi\Omega/V_p \approx \varpi/\varpi_{\rm LC}$.

For a rotating BH-jet

$$\frac{|B_\phi|}{B_z} \approx 150 \left(\frac{r_j}{10^{16}{\rm cm}}\right)\left(\frac{\varpi_{\rm LC}}{4GM/c^2}\right)^{-1}\left(\frac{M}{10^8 M_\odot}\right)^{-1}$$

For a disk-jet $\frac{|B_\phi|}{B_z} \approx 20 \left(\frac{r_j}{10^{16}{\rm cm}}\right)\left(\frac{r_0}{10GM/c^2}\right)^{-3/2}\left(\frac{M}{10^8 M_\odot}\right)^{-1}$

Strong B_ϕ induces current-driven instabilities (Kruskal-Shafranov)

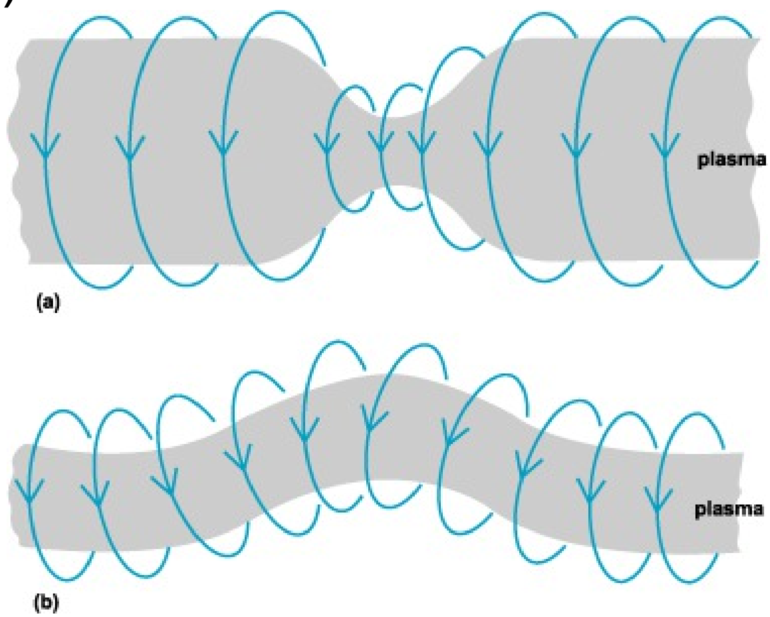

Interaction with the environment $\rightarrow$ Kelvin-Helmholtz instabilities

Stability of axisymmetric solutions (analytical or numerical)? Role of B_z? of inertia?

Relation with observations? (knot structure, jet bending, shocks, polarization degree, reconnection)

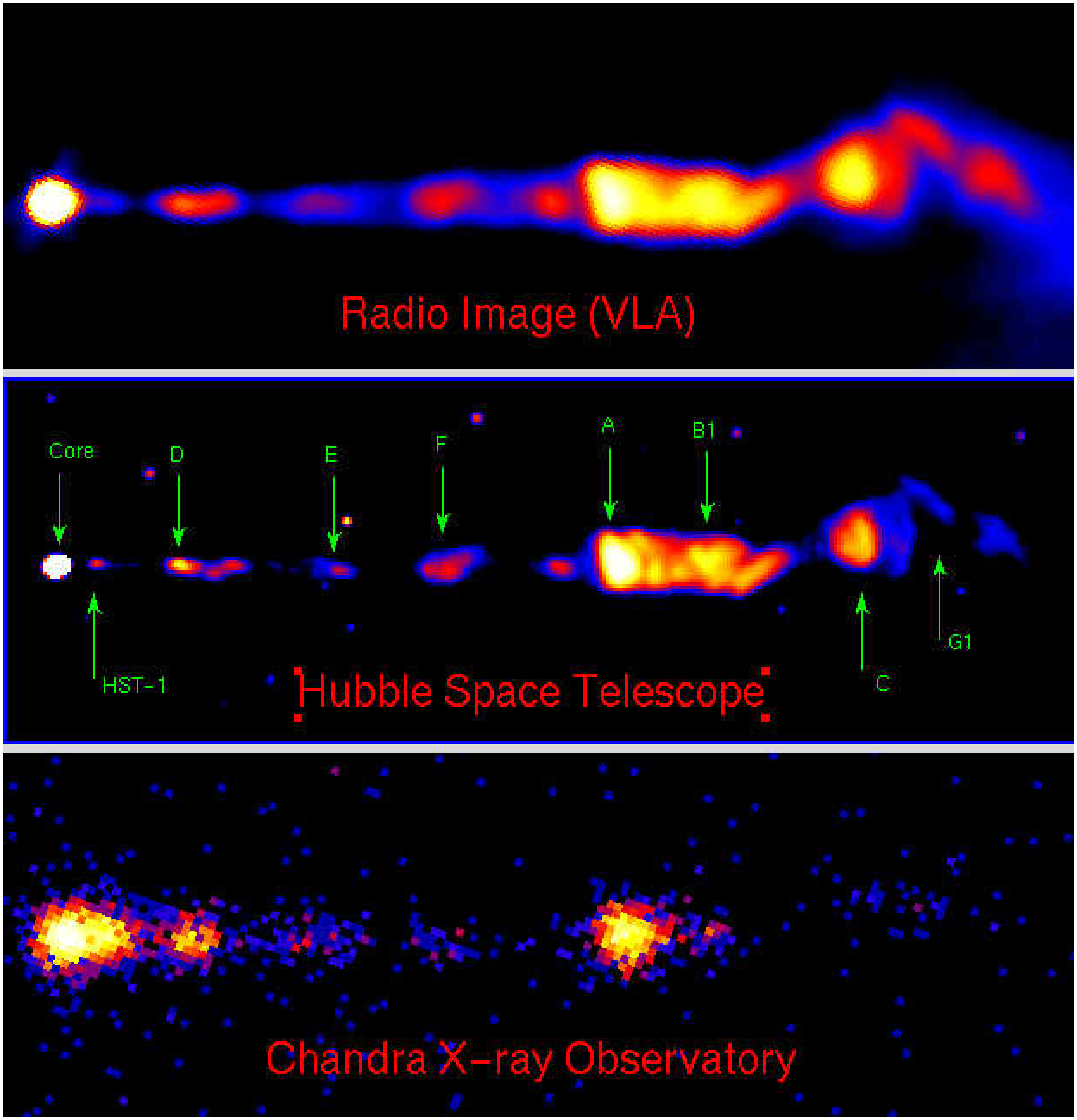
Radio Image (VLA)
Core
D
E
F
A
B1
HST-1
Hubble Space Telescope
C
G1
Chandra X-ray Observatory

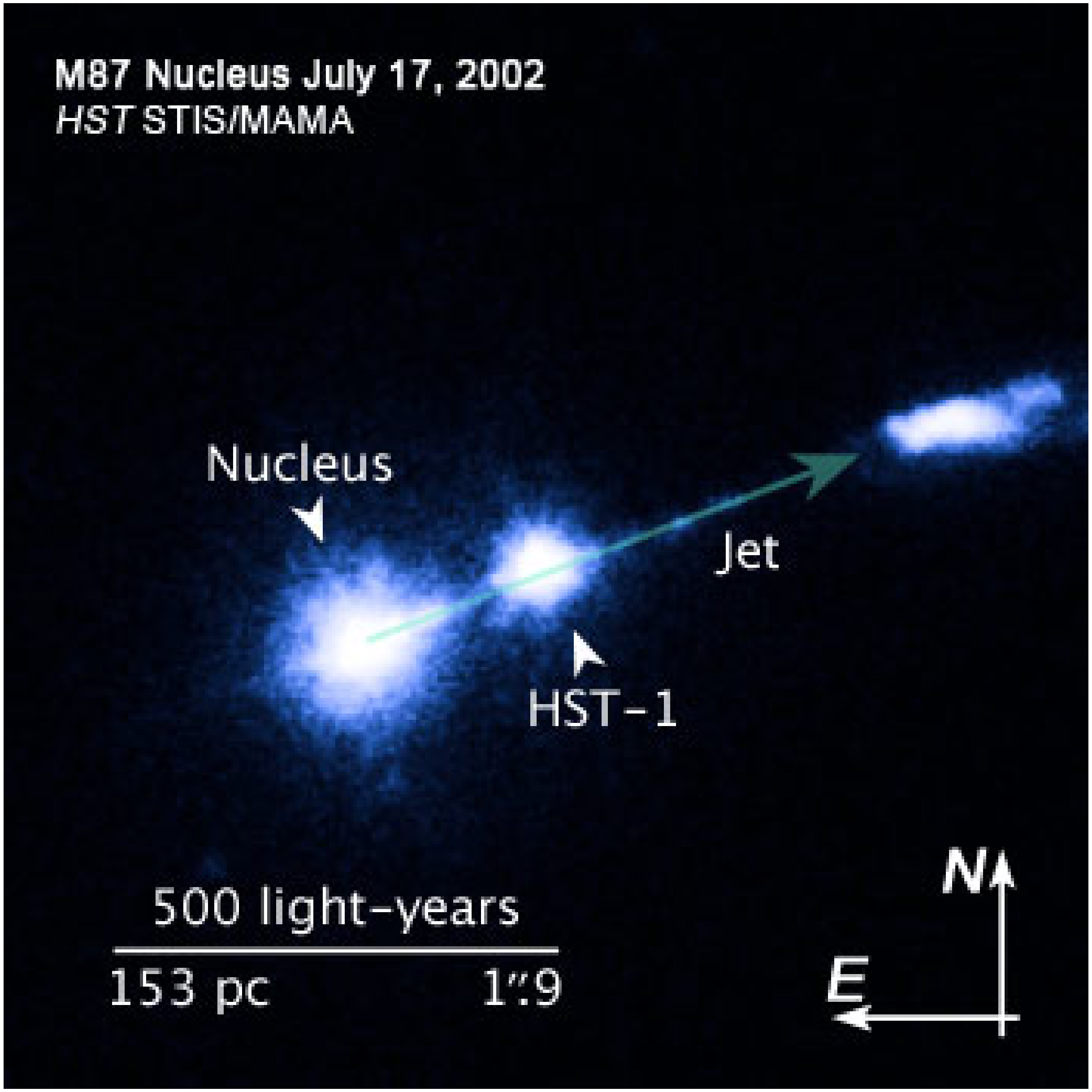
M87 Nucleus July 17, 2002
HST STIS/MAMA
Nucleus
Jet
HST-1
500 light-years
153 pc
1''.9
N
E

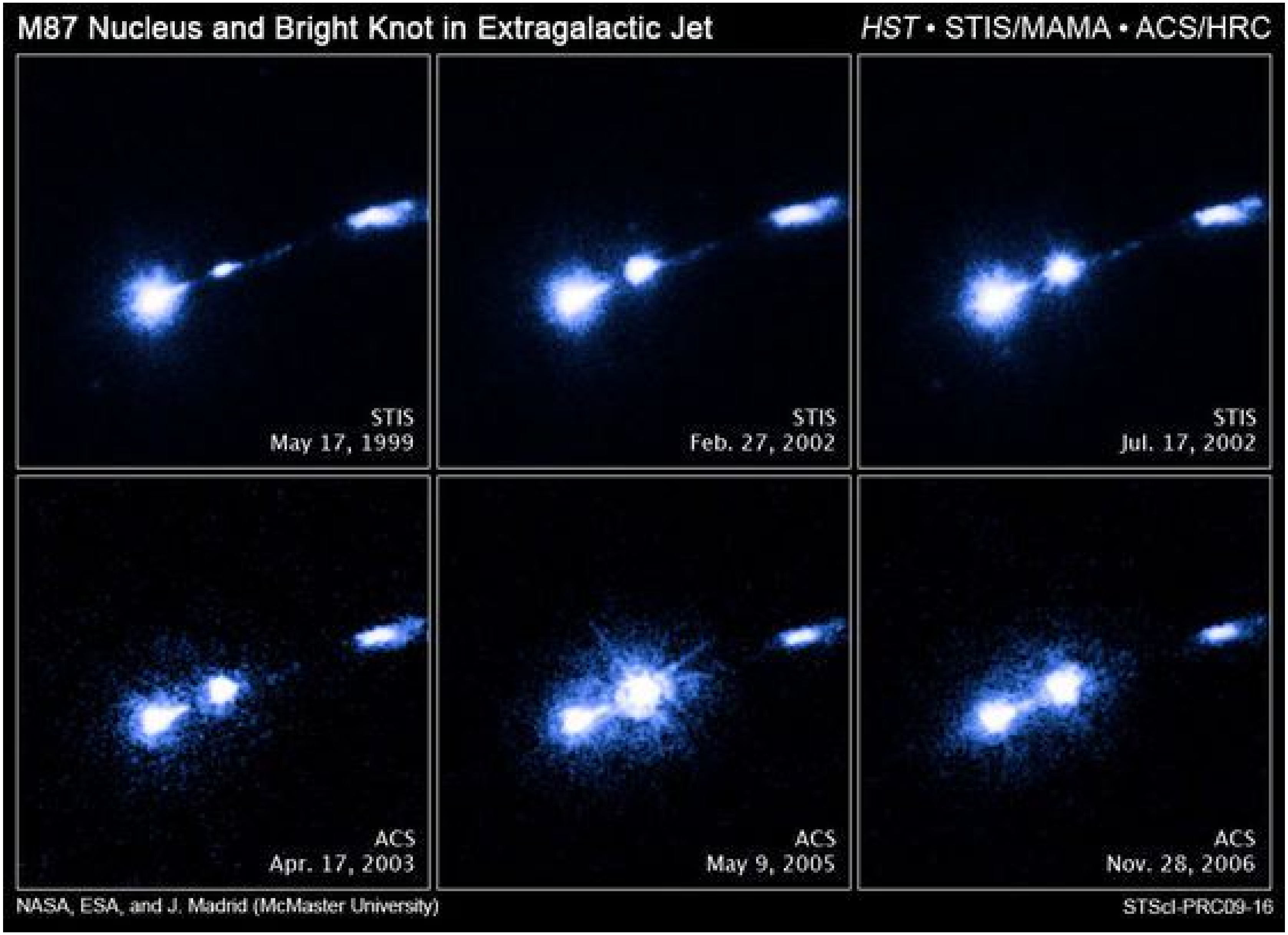
M87 Nucleus and Bright Knot in Extragalactic Jet
HST • STIS/MAMA • ACS/HRC
STIS
May 17, 1999
STIS
Feb. 27, 2002
STIS
Jul. 17, 2002
ACS
Apr. 17, 2003
ACS
May 9, 2005
ACS
Nov. 28, 2006
NASA, ESA, and J. Madrid (McMaster University)
STScI-PRC09-16

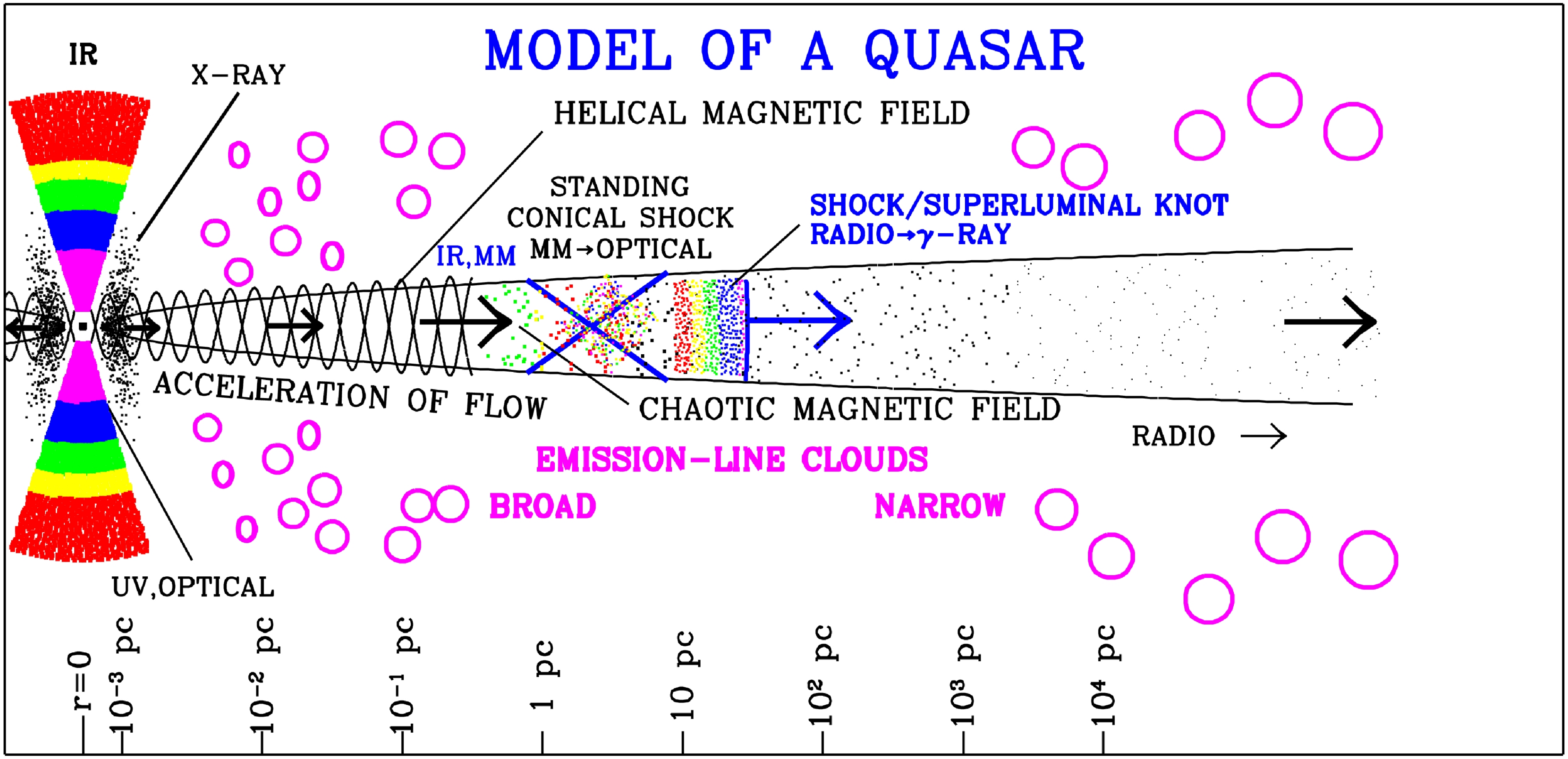
MODEL OF A QUASAR
IR
X-RAY
HELICAL MAGNETIC FIELD
STANDING
CONICAL SHOCK
MM→OPTICAL
IR,MM
SHOCK/SUPERLUMINAL KNOT
RADIO→γ-RAY
ACCELERATION OF FLOW
CHAOTIC MAGNETIC FIELD
RADIO →
EMISSION-LINE CLOUDS
BROAD
NARROW
UV,OPTICAL
r=0
10⁻³ pc
10⁻² pc
10⁻¹ pc
1 pc
10 pc
10² pc
10³ pc
10⁴ pc

Stability analysis

- Are astrophysical jets stable? (contrary to lab jets)

- 3D relativistic MHD simulations hard to cover the full jet range (formation and propagation zone + environment)

interesting results for the jet-formation region (McKinney & Blandford, Tchekhovskoy, Narayan & McKinney)

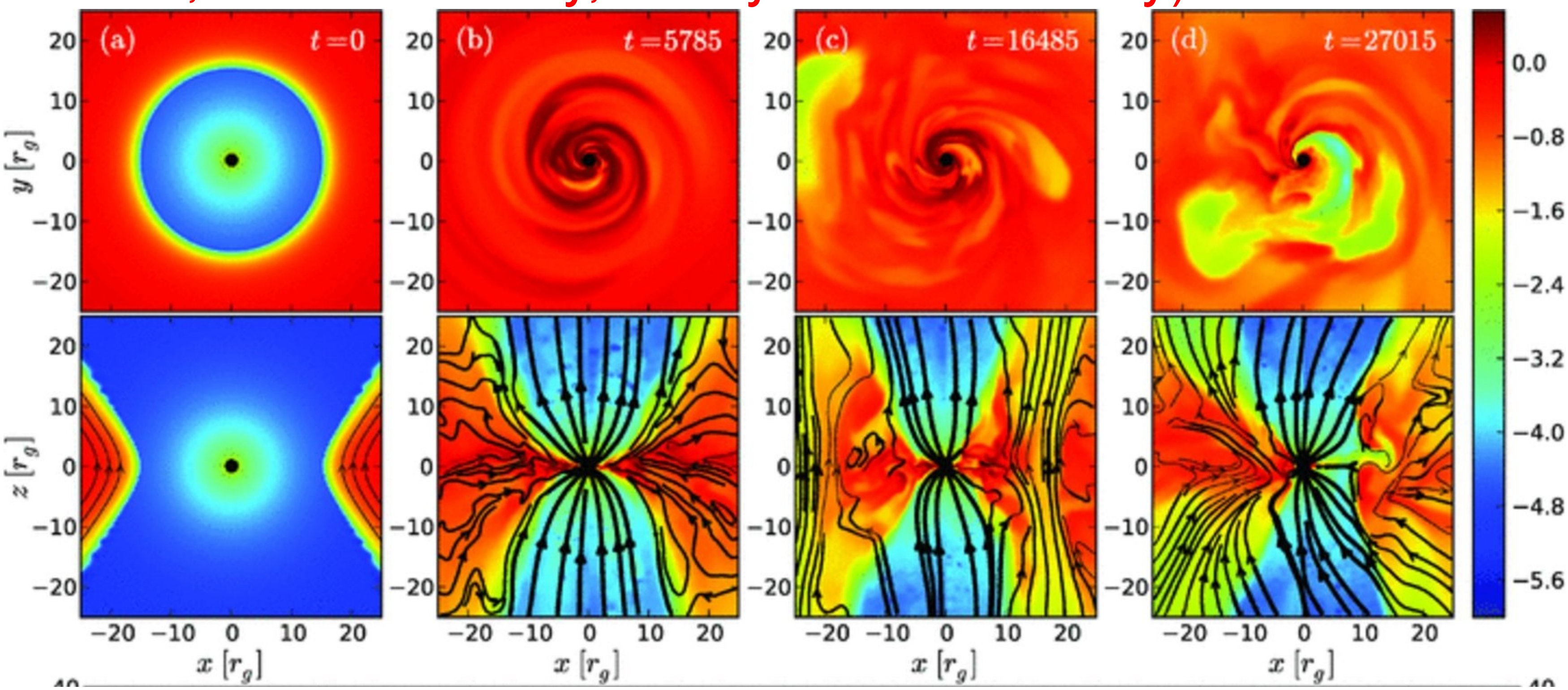

Linear Stability Analysis

Unperturbed flow: Cylindrical jet

helical, axisymmetric, cylindrically symmetric and steady flow

$$\boldsymbol{V}_0 = V_{0z}(\varpi)\hat{z} + V_{0\phi}(\varpi)\hat{\phi}\,,$$

$$\boldsymbol{B}_0 = B_{0z}(\varpi)\hat{z} + B_{0\phi}(\varpi)\hat{\phi}\,, \quad \boldsymbol{E}_0 = -\frac{\boldsymbol{V}_0 \times \boldsymbol{B}_0}{c}\,,$$

$$\rho_{00} = \rho_{00}(\varpi)\,, \quad \xi_0 = \xi_0(\varpi)\,,$$

$$\Pi_0 = \frac{\Gamma - 1}{\Gamma}\left(\xi_0 - 1\right)\rho_{00}c^2 + \frac{B_0^2 - E_0^2}{8\pi}\,.$$

Equilibrium condition

$$\frac{B_{0\phi}^2 - E_0^2}{4\pi\varpi} - \xi_0\rho_{00}\frac{\gamma_0^2 V_{0\phi}^2}{\varpi} + \frac{d\Pi_0}{d\varpi} = 0\,.$$

Linearized equations

$$Q(\varpi\,,z\,,\phi\,,t) = Q_0(\varpi) + Q_1(\varpi)\exp\left[i(m\phi + kz - \omega t)\right]$$

$$\left(\begin{array}{c} 10\times 12 \text{ array} \\ \text{function of } \varpi\,,\omega\,,k \end{array}\right)\left(\begin{array}{c} \gamma_1 \\ \rho_{01} \\ B_{1z} \\ B_{1\phi} \\ iB_{1\varpi} \\ \xi_1 \\ V_{1z} \\ V_{1\phi} \\ d\left(i\varpi V_{1\varpi}\right)/d\varpi \\ d\Pi_1/d\varpi \\ i\varpi V_{1\varpi} \\ \Pi_1 \end{array}\right) = 0$$

reduces to (4 equations in real space)

$$\frac{d}{d\varpi}\begin{pmatrix} y_1 \\ y_2 \end{pmatrix} + \frac{1}{\mathcal{D}}\begin{pmatrix} \mathcal{F}_{11} & \mathcal{F}_{12} \\ \mathcal{F}_{21} & \mathcal{F}_{22} \end{pmatrix}\begin{pmatrix} y_1 \\ y_2 \end{pmatrix} = 0\,,$$

where the (complex) unknowns are

$$y_1 = i\frac{\varpi V_{1\varpi}}{\omega_0}\,, \qquad y_2 = \Pi_1 + \frac{y_1}{\varpi}\frac{d\Pi_0}{d\varpi}$$

($\mathcal{D}\,, \mathcal{F}_{ij}$ are determinants of 10×10 arrays).

Equivalently

$$y_2'' + \left[\frac{\mathcal{F}_{11}+\mathcal{F}_{22}}{\mathcal{D}} + \frac{\mathcal{F}_{21}}{\mathcal{D}}\left(\frac{\mathcal{D}}{\mathcal{F}_{21}}\right)'\right] y_2' + \left[\frac{\mathcal{F}_{11}\mathcal{F}_{22}-\mathcal{F}_{12}\mathcal{F}_{21}}{\mathcal{D}^2} + \frac{\mathcal{F}_{21}}{\mathcal{D}}\left(\frac{\mathcal{F}_{22}}{\mathcal{F}_{21}}\right)'\right] y_2 = 0\,,$$

which for uniform flows with $V_{0\phi}=0$, $B_{0\phi}=0$, reduces to Bessel.

Eigenvalue problem

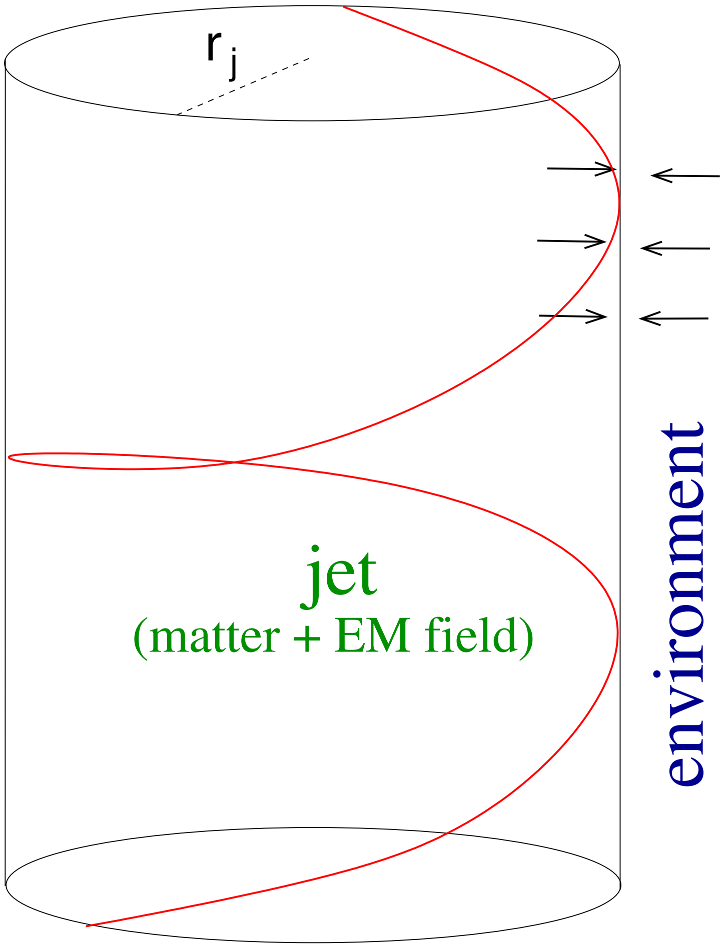

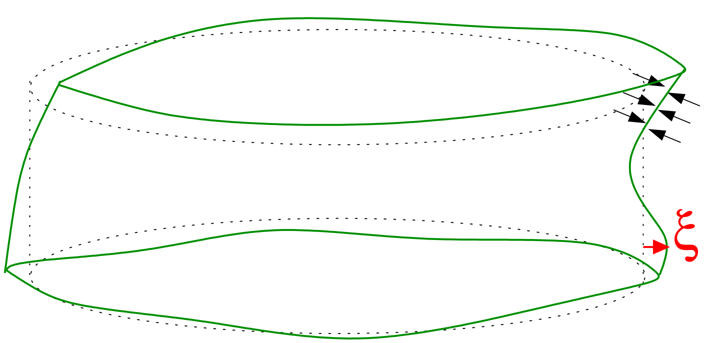

- solve the problem inside the jet (attention to regularity condition on the axis)

- similarly in the environment (solution vanishes at ∞)

- Match the solutions at r_j:

$[\![y_1]\!] = 0\,, [\![y_2]\!] = 0 \longrightarrow$ dispersion relation

$\star$ spatial approach: $\omega = \Re\omega$ and $\Re k = \Re k(\omega), \Im k = \Im k(\omega)$

$$Q = Q_0(\varpi) + Q_1(\varpi) e^{-\Im k z} e^{i(m\phi + \Re k z - \omega t)}$$

$\star$ temporal approach: $k = \Re k$ and $\Re\omega = \Re\omega(k), \Im\omega = \Im\omega(k)$

$$Q = Q_0(\varpi) + Q_1(\varpi) e^{\Im\omega t} e^{i(m\phi + kz - \Re\omega t)}$$

Sinnis & Vlahakis in preparation

temporal analysis of a cold, nonrotating jet

- γ_0 , ρ_{00} constants

- $B_{0z} = \dfrac{B_0}{1+(\varpi/\varpi_0)^2}$, $\quad B_{0\phi} = B_{0z}\dfrac{\varpi}{\varpi_0}$,

- ϖ_0 controls $\dfrac{B_\phi}{B_z}$ and B_0 the magnetization $\sigma = \dfrac{B_\phi^2/\gamma^2}{4\pi\rho_0}$

- external medium: uniform, static, unmagnetized

density ratio η (external over axial)
(We also solved for cold, uniformly magnetized environments.)

- pressure equilibrium at jet surface

What to expect

nonrelativistic linear studies predict growth rates (in comoving frame) $\Gamma_{\rm co} \sim \frac{v_A}{10\varpi_0}$ (Appl et al)

in the lab frame $\Gamma = \frac{\Gamma_{\rm co}}{< \gamma >}$

for typical values $v_A = \sqrt{\frac{\sigma}{\sigma+1}} \sim 1, \quad \varpi_0 \sim 0.1\varpi_j, \quad < \gamma > \sim 5$
the growth rate is $\sim 0.2c/\varpi_j$

typical growth times $\sim 5\varpi_j/c$

nonlinear effects become important after a few $10\varpi_j$

Results (Re=solid, Im=dashed)

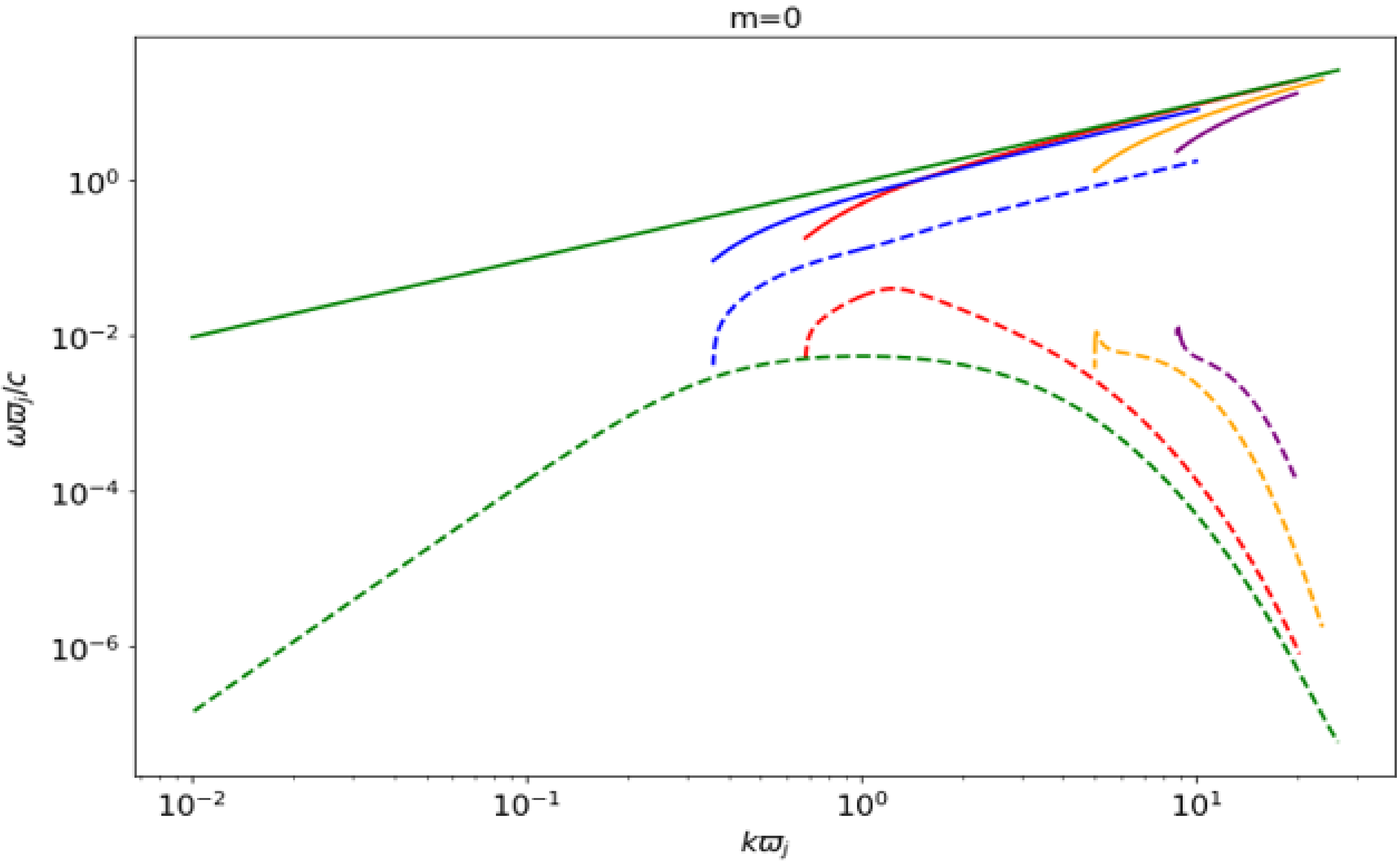

A hyper-unstable mode appears!

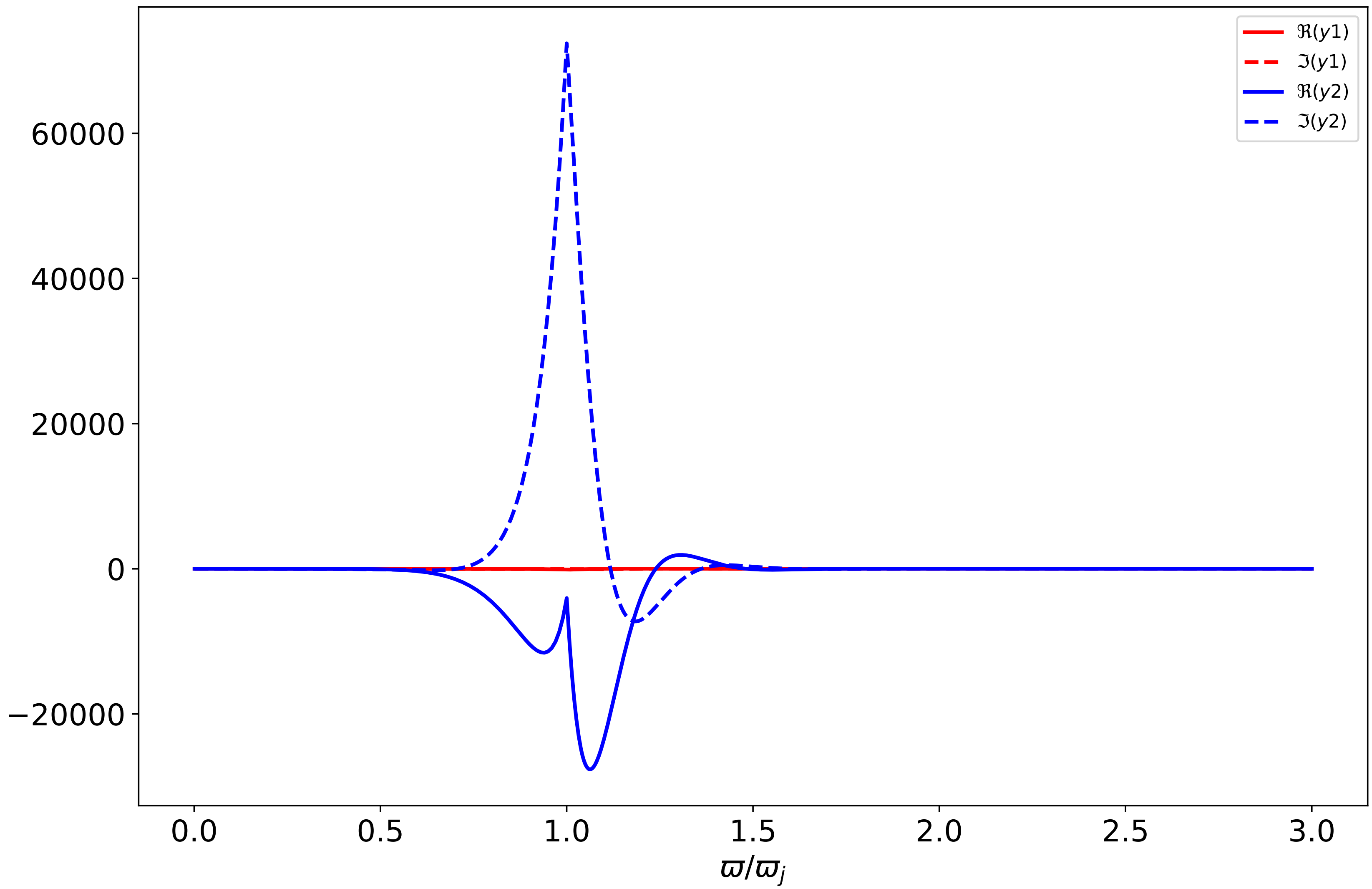
$\Re(y1)$
$\Im(y1)$
$\Re(y2)$
$\Im(y2)$
60000
40000
20000
0
−20000
0.0
0.5
1.0
1.5
2.0
2.5
3.0
ϖ/ϖ_j

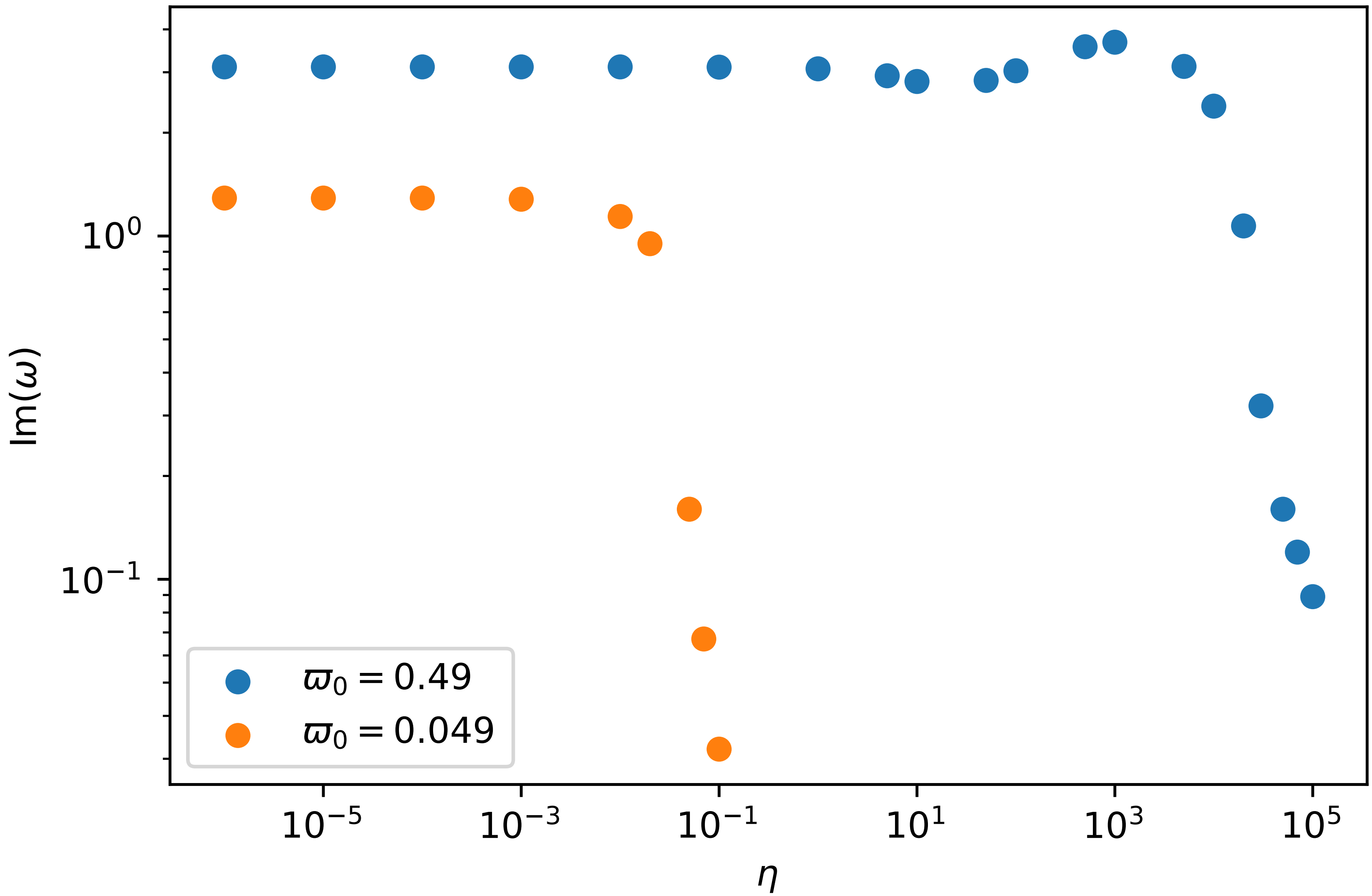
10^0
10^{-1}
10^{-5}
10^{-3}
10^{-1}
10^1
10^3
10^5
η
$\mathrm{Im}(\omega)$
$\varpi_0 = 0.49$
$\varpi_0 = 0.049$

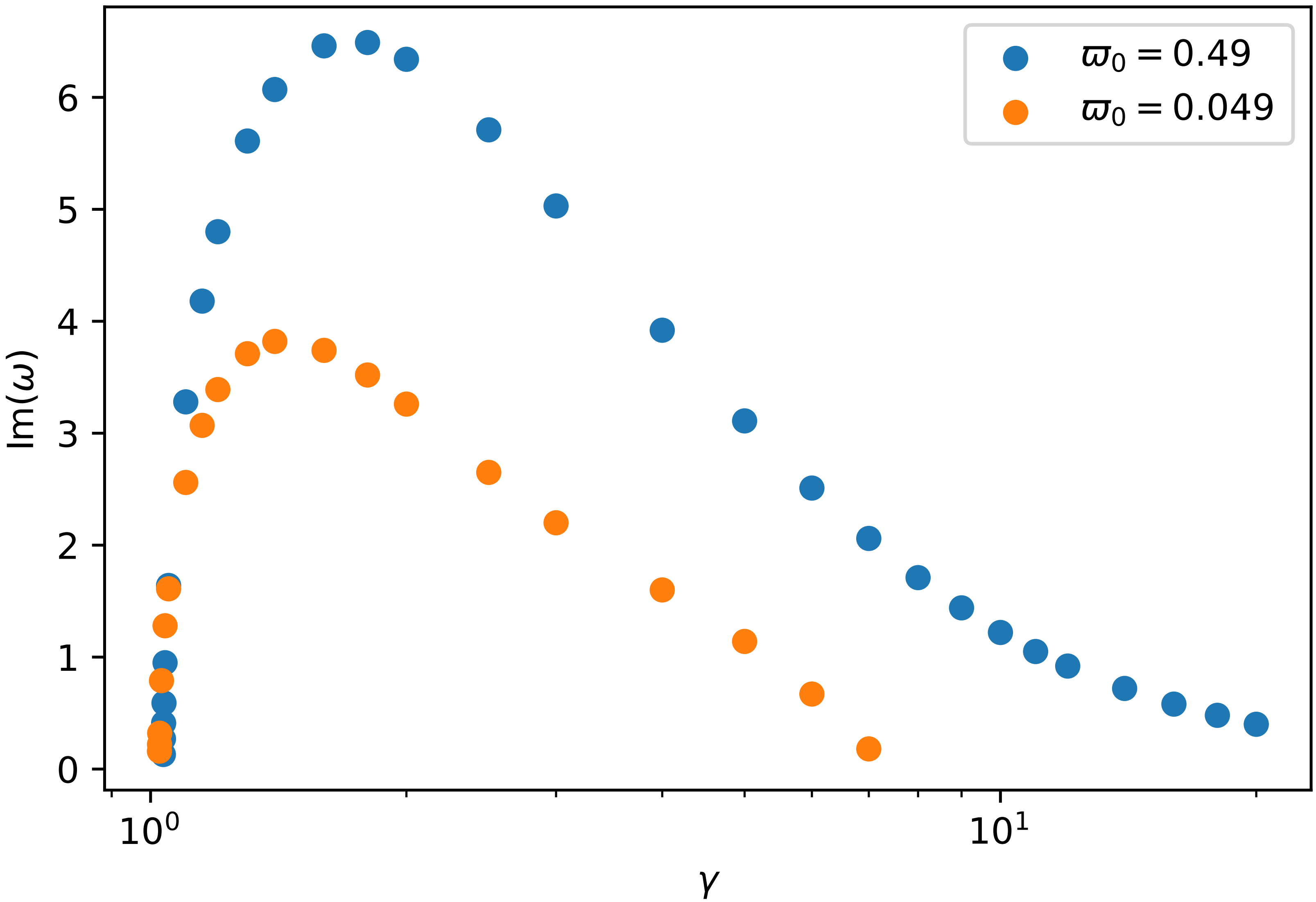

$\varpi_0 = 0.49$
$\varpi_0 = 0.049$
6
5
4
3
2
1
0
Im(ω)
10^0
10^1
γ

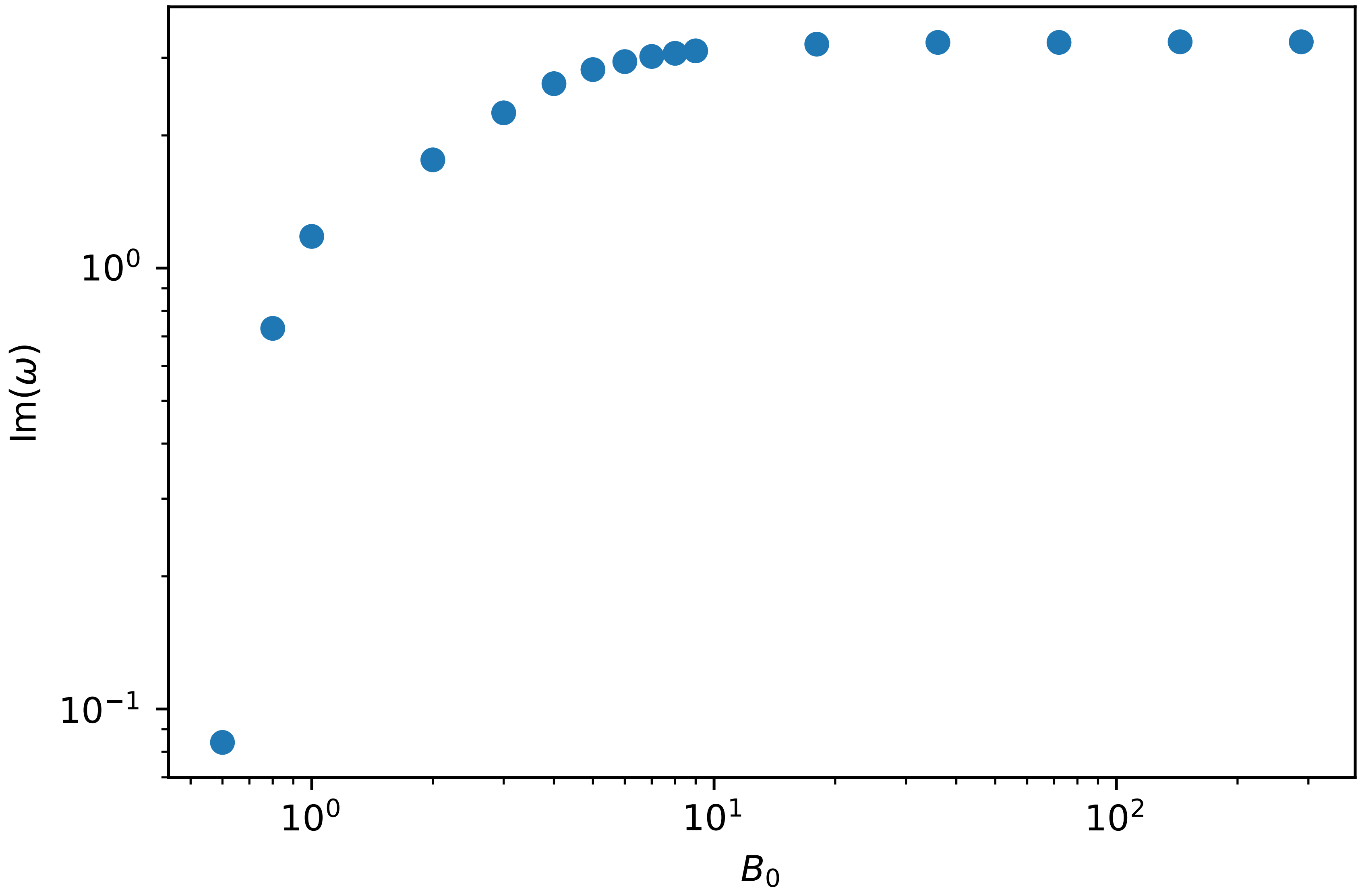

10^0
10^{-1}
$\mathrm{Im}(\omega)$
10^0
10^1
10^2
B_0

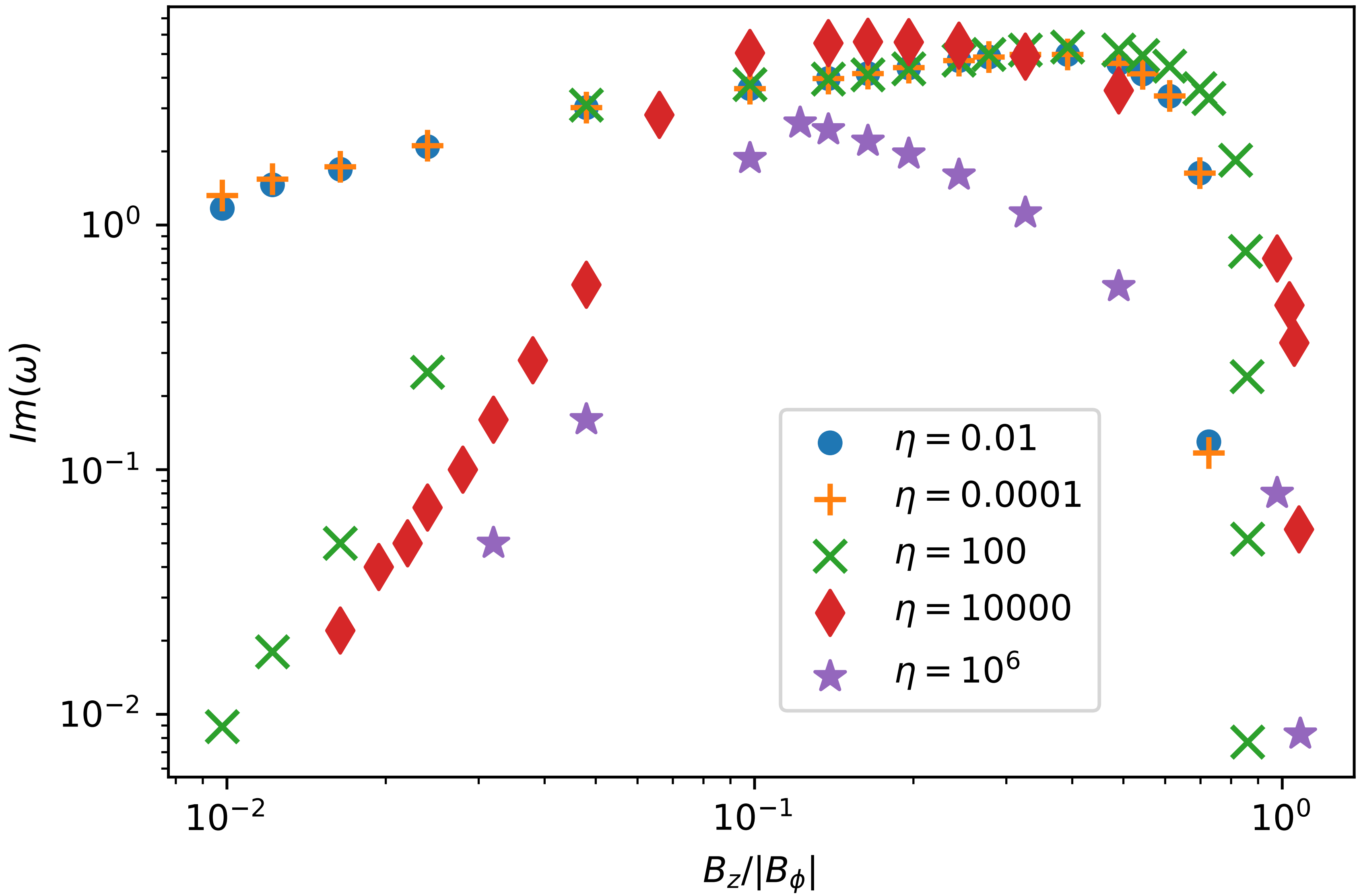
$Im(\omega)$
10^0
10^{-1}
10^{-2}
10^{-2}
10^{-1}
10^0
$B_z/|B_\phi|$
$\eta = 0.01$
$\eta = 0.0001$
$\eta = 100$
$\eta = 10000$
$\eta = 10^6$

Summary

- $\star$ magnetic field + rotation $\rightarrow$ Poynting flux extraction
- $\star$ the collimation-acceleration mechanism is very efficient – provides a viable explanation for the bulk acceleration in all jets (relativistic or not)
- $\star$ acceleration efficiency $\gtrsim 50\%$
- $\star$ environment significantly affects jet dynamics in the acceleration-collimation zone (jet-shape, spatial scale of γ)

- ⋆ typical instability growth length = a few tens ϖ_j
  volume or surface instabilities

- ⋆ a hyper-unstable surface mode tends to appear for heavy jets with mildly relativistic speeds, high magnetizations, only for $B_z < |B_\phi|$

- ⋆ interesting to analyze the nonlinear evolution via simulations (preliminary results show that the jet relaxes to a new quasi-steady-state)

Thank you for your attention